Fractal Pennes and Cattaneo-Vernotte Bioheat Equations from Product-Like Fractal Measure and their Implications in Cells Tissues with Tumor Growth

Rami Ahmad El-Nabulsi
Research Center for Quantum Technology, Faculty of Science, Chiang Mai University, Chiang Mai, 50200, Thailand
Department of Physics and Materials Science, Faculty of Science, Chiang Mai University, 50200, Thailand
Athens Institute for Education and Research, Mathematics and Physics Divisions, 8 Valaoritou Street, Kolonaki, 10671, Athens, Greece
Personal Emails: el-nabulsi@atiner.gr, nabulsiahmadrami@yahoo.fr

Abstract

In this study, the Pennes and Cattaneo-Vernotte bioheat transfer equations in the presence of fractal spatial dimensions are derived based on the product-like fractal geometry. This approach was introduced recently, by Li and Ostoja-Starzewski, in order to explore dynamical properties of anisotropic media. The theory is characterized by a modified gradient operator which depends on two parameters: R which represents the radius of the tumor, and R_0 which represents the radius of the spherical living tissue. Both the steady and unsteady states for each fractal bioheat equations were obtained and their implications on living cells in the presence of a large tumor growth were analyzed. Assuming a specific heating/cooling by a constant heat flux equivalent to the metabolic heat generation in the tissue, it was observed that the solutions of the fractal bioheat equations are robustly affected by fractal dimensions, the radius of the tumor growth and the dimension of the living cell tissue. The ranges of both the fractal dimension and temperature were obtained, analyzed, and compared with recent studies. This study confirms the importance of fractals in medicine.

Keywords: product-like fractal measure; fractal bioheat equation; cell tissues
Pacs Numbers: 87.10.+e; 87.17.-d

1. Introduction

Kinetic theory is one of the most important fields in statistical physics due to its large implications in the understanding of various complex phenomena such as radiative transfer, polymer flows, quantum hydrodynamics, diffusion processes, cellular mechanics, and phase transitions [**1**]. Its formalism can be developed for both classical and quantum dynamical systems. Recently, the concept of kinetic theory has been extended to fractal systems due to the importance of fractals in nearly all fields of sciences and engineering [**2,3**]. Fractal kinetic theory has been explored in surface chemical reactions [**4**], spin dynamics [**5**], adsorption on mesoporous carbons [**6**], reaction kinetics of proteins and enzymes [**7**], diffusion-limited reactions [**8-10**], non-extensive thermodynamics [**11**], rock fractures in fluid flows [**12**], colloid science [**13**], fluids dynamics simulations [**14**], porous media [**15**], among others. More generally, fractals have imperative implications in materials sciences [**16**], fluids flows [**17,18**], elastic and continuum media [**19**], electromagnetic theory [**20,21**], quantum mechanics [**22-26**], astrophysics [**27-36**], fluid mechanics and nanofluid [**37,38**], transport in complex porous media [**39**], materials sciences [**40**], heat transfer [**41**], etc.

Mathematically, fractals are the generic models generated by scaling equations which emerge in chaotic dynamical systems. Although their complex and intricate structures, fractals are also artistic and they are defined by a recursive process characterized by self-similarities and fractal dimensions. Fractals are very important in biological systems where shapes are very important at mesoscopic scales, e.g. diffusion of gas through the fractal landscape of the lung and quantification of oocyte cytoplasm morphology. Fractals emerge also in neurosciences where they play a leading role in the scaling analysis of cerebral hemodynamics and the modeling of human gait. Moreover, they arise in tumors cells and they are used in the analysis of vascular network pattern in human diseases and canine trichoblastoma (see [**42**] for a good review). It is notable that our circulatory blood system, brains, arteries, veins, rhythms of heartbeats, walking strides, biological changes of aging, bronchioles and our lungs are characterized by fractals patterns [**43**]. The bronchial tubes in our lung and kidneys are characterized by one fractal dimension for the first seven generations of branching

[**44**]. Besides, fractal geometry is at the leading edge of research in understanding the function of our brains [**45,46**].

In medical research fractals are largely involved in the understanding of several biological aspects such as the dynamics and the propagation of bacteria and virus on the surfaces of our bodies [**47**]. As for the AIDS virus, it has been observed that their dynamics in the human body may be successfully modeled by means of fractals and hence provides a natural explanation to the long-standing puzzle encountering the abnormally long incubation stage of the AIDS virus [**48**]. Moreover, fractals have been used in the detection of cancer cells and cystic fibrosis in human bodies [**49**]. Fractal geometry has been applied in the therapeutic of breakable bone fractures [**50**], in modeling of lung morphogenesis [**51**], in physiology [**52**], in vascular biology [**53**], in microbiology [**54**] among several domains in medicine including pathology, oncology, and radiographic diagnostic [**55-63**].

However, in most biological systems and biological materials, anisotropy is an essential feature [**64**]. Anisotropy has important implications in anisotropic optical biological network [**65,66**], biological tissues [**67**], DNA-mediated anisotropic mechanical reinforcement of a virus [**68**], measurement of bone texture radiographs [**69**], post-menopausal osteoporosis and trabecular bone radiographic images [**70**] and in disruption of tissue architecture/cancer [**71**]. Although isotropic and anisotropic fractals were largely explored in biology and medicine, the formulation of kinetic theory in anisotropic biology characterized by fractal dimensions is still not well elaborated in literature. Modelling complex biological systems by means of the conventional mathematical kinetic theory was done in literature [**72**] yet the standard analysis is unable to portray a variety of fractal geometrical structures emerging in biology and medicine since biological systems are at the present time lengthily understood as being inherently fractal. This is the main reason why nowadays there is an interest in fractal pharmacokinetics [**73,74**].

In the present study, we would like to construct an anisotropic kinetic theory in fractal dimensions staring from a completely dissimilar fractal perspective known by the concept of "product-like fractal geometry" which was introduced by Li and Ostoja-Starzewski in [**75**] and entitled LOSA (Li and Ostoja-Starzewski approach). This approach describes fruitfully the nonlinear dynamics and the physics in anisotropic fractal-dimensional media [**76-82**] and has a series of motivating implications in various fields of sciences and engineering [**83-86**]. Given that LOSA is productively used in anisotropic media, it will be of interest to explore its implications in kinetic biology. It is very important to understand the role of heat and thermodynamics in biological systems, e.g. energy flow [**87**], nonequilibrium thermodynamics of living organisms such as mitochondria and energy transduction in the mitochondrion [**88,89**], thermodynamics of growth and microorganisms [**90**], bioengineering thermodynamics of biological cells [**91**], etc. Cells in our body are well-organized and their corresponding entropy is very low. However, to maintain this order, energy is lost to the environment or transformed. This process results in an increase in entropy in the cell's/organism's surroundings [**92**].

Given the importance of these topics, it will be of interest to describe the fractal transfer of temperature or internal pressure in tumor growth. The study of temperature or internal pressure in tumor growth is significant for hyperthermia or thermal ablation which uses thermal energy deposited to exterminate cancer cells (i.e., coagulation necrosis) with minimal injury to normal tissue [**93-96**]. Although the mathematical models

discussed in literature which are based on fractals geometry have proved to be practical to imitate the growth of tumor cell number over time [**96-98**], the implications of a fractal kinetic theory in tumor growth is still not well-completed. This will be the main focus of the present study. As mentioned previously, the solutions of fractal bio-heat transfer problems are important in biomedical applications such as the ones for thermo-therapeutic treatment.

This study is organized as follows: in **Sec. 2**, we review the basic setups of LOSA and then, we formulate the fluid kinetic equations where we introduce the fractal advection-diffusion equation which will be recognized as the fractal Pennes bioheat transfer equation; in **Sec. 3**, we discuss the steady-state solution and its main implications in cell tissues in the presence of a tumor growth; in **Sec. 4**, the time-dependent solutions are derived and discussed; and finally, conclusions are given in **Sec. 5**.

2. LOSA, Fractal Kinetic Theory and Fractal Pennes Bioheat Transfer Equation

Before we introduce the fractal Pennes bioheat transfer equation, we briefly review the basic formalism of LOSA. This new fractal approach is, in fact, based on simple geometrical arguments: given a parallelepiped of lengths x_1, x_2, x_3, mass $m = m(x_1, x_2, x_3)$ and density $\rho = \rho(x_1, x_2, x_3)$ on a fractal set W having dimension $D = \alpha_1 + \alpha_2 + \alpha_3$ with $0 < \alpha_k \le 1$. Li and Ostoja-Starzewski set up the following conceivable characterization of its mass distribution through a product measure: $m = \int_V \rho \prod_{k=1}^{3} d\mu_k(x_k), k = 1,2,3$ where $d\mu_k(x_k) := c_1^k(\alpha_k, x_k) dx_k$ is the length measurement with $c_1^{(k)}(\alpha_k, x_k) = \alpha_k((l_k - x_k)/l_{k0})^{\alpha_k - 1}$, $0 < x_k < l_k$ obtained through the modified Riemann-Liouville fractional integral [**86**]. l_k is the length along axis x_k and l_{k0} is a characteristic length. In general, $c_3 = \prod_{i=1}^{3} c_1^{(i)}$ is the volume coefficient of the parallelepiped and $(c_1^{(1)})^{-1} = \alpha(l_0/(l - x))^{\alpha - 1}$.

In this context, the operators gradient and Laplacian are generalized to their fractal counterparts as follows: $\nabla_k^D = (c_1^{(k)})^{-1} \nabla_k$ and $\Delta_k^D = \nabla_k^D \cdot \nabla_k^D$. ∇ and Δ are the conventional gradient and Laplacian operators respectively. It is notable that both the Stokes theorem $\int_A \mathbf{n} \cdot \nabla \times f dS_d = \int_l \mathbf{f} \cdot dl_{\alpha_1}$ and the divergence theorem $\int_V \nabla^D \cdot \mathbf{f} dV_D = \int_S \mathbf{f} \cdot \mathbf{n} dS_d$ still hold. Here $\nabla^D = \mathbf{e}_k \nabla_k^D$, $\mathbf{e}_k$ are base vectors, $dV_D = \prod_{k=1}^{3} c_1^{(k)} dV$ is the infinitesimal fractal volume element, $dS_d^{(k)} = dx_i dx_j$ such that $dS_d^{(k)} = c_2^{(k)} dS_2$ where $c_2^{(k)} = c_1^{(i)} c_1^{(j)} = c_3 / c_1^{(k)}, i \ne j, i, j \ne k$. In this framework, $d^{(k)} = \alpha_i + \alpha_j$ is the fractal dimension of the surface $S_d^{(k)}$ along the diagonals $|x_i| = |x_j|$ in $S_d^{(k)}$. It is noteworthy that LOSA still holds in radial coordinates since one can define the fractal derivative (or the fractal gradient) operator by $\frac{\partial}{\partial r} := \nabla_r \to \nabla_r^\alpha = (\frac{R_0}{R - r})^{\alpha - 1} \nabla, 0 < r < R$ with R being the length along radial axis r and R_0 is a typical length. One of the main advantages of LOSA is its association with conventional analysis and the decoupling of coordinate variables through coefficients c_1, c_2 and c_3 which overpoweringly simplifies the Gauss theorem.

Our starting point is basically the Hamiltonian dynamics for N identical point particles. The Hamiltonian of a particle of mass m located at position $\mathbf{r}_i$ at time t takes the form:

$$H = \frac{1}{2m} \sum_{i=1}^{N} \left(\mathbf{p}_i^2 + V(\mathbf{r}_i) \right) + \sum_{i<j} U\left(\mathbf{r}_i - \mathbf{r}_j \right), \tag{1}$$

Here V is the potential, $\mathbf{p}$ is the momentum of the body and $U(\mathbf{r}_i - \mathbf{r}_j)$ is the potential energy due to the two-body interactions between particles. We assume that the Hamiltonian contains an external force $\mathbf{F} = -\nabla^D V$ acting equally on all particles. The associated Hamilton's equations of the system are: $\dot{\mathbf{p}}_i = -\nabla_i^D H$ and

$\dot{\mathbf{r}}_i = \partial H / \partial \mathbf{p}_i$. Here "dot" represents the derivative with respect to time. We recall that, in this study, we have considered only spatial fractal dimensions and therefore the fractal gradient operator acts only in the space of generalized coordinates.

Remark 2.1: *It is well-known that in classical mechanics, the velocity of a particle can be specified either in terms of Cartesian coordinates or in terms of generalized coordinates. In Cartesian coordinates, the velocity of the body is given by* $v_i \equiv \dot{x}_i$ *. However, for* $x_i = x_i(q_1, q_2, q_3, t)$ *, it is easy to verify that*: $v_i \equiv \dot{x}_i = \sum_{k=1}^{3} (\nabla_k^D x_i)\dot{q}_k + \dot{x}_i$ *where* $\nabla_k^D := (c_1^{(k)})^{-1} \nabla_k = (c_1^{(k)})^{-1} \partial / \partial q_k$ *Using the fact that a mixed second-order partial derivative is independent of the order of the derivatives and that* $\partial x_i / \partial \dot{q}_j = 0$ *, we find*:

$$\frac{\partial v_i}{\partial \dot{q}_j} \equiv \frac{\partial}{\partial \dot{q}_j} \sum_k \left(\nabla_k^D x_i \right) \dot{q}_k + \frac{\partial \dot{x}_i}{\partial \dot{q}_j} = \frac{\partial}{\partial \dot{q}_j} \sum_k \left(\nabla_k^D x_i \right) \dot{q}_k = \sum_k \left(\frac{\partial}{\partial \dot{q}_j} \nabla_k^D x_i \right) \dot{q}_k + \sum_k \nabla_k^D x_i \frac{\partial \dot{q}_k}{\partial \dot{q}_j},$$

$$= \sum_k \nabla_k^D x_i \frac{\partial \dot{q}_k}{\partial \dot{q}_j} = \sum_k \nabla_k^D x_i \delta_{ij} = \nabla_j^D x_i .$$

This states that in LOSA, the Cartesian velocity is connected to the generalized velocity in a similar manner as the Cartesian coordinate is related to the generalized coordinate [**99**].

Let $f(\mathbf{r}_i, \mathbf{p}_i, t)$ be a normalized classical distribution function over the $6N$ dimensional phase space that represents the probability of finding a particle of mass m located at position $\mathbf{r}_i$ at time t . This function is assumed to hold at nonequilibrium state. The fractal continuity equation/Liouville equation of the probability distribution is given by:

$$\frac{\partial f}{\partial t} + \{H, f\}_D = 0 , \tag{2}$$

where

$$\{H, f\}_D = \nabla_i^D f \frac{\partial H}{\partial \mathbf{p}_i} - \frac{\partial f}{\partial p_i} \nabla_i^D H . \tag{3}$$

Several well-known partial differential equations may be obtained subsequently. In particular, if ρ is the density of the body moving with vector velocity $\mathbf{u} = \mathbf{u}(u, v, w)$ within the elementary volume dV and assumed to be of elementary mass $dm = \rho dxdydz = \rho dV$, then the following fractal continuity equation holds accordingly [**84**]:

$$\left(\frac{D\rho}{Dt} \right)_D + \rho \nabla^D \cdot \mathbf{u} = 0 , \tag{4}$$

where $\left(\frac{D}{Dt} \right)_\alpha = \frac{\partial}{\partial t} + \mathbf{u} \cdot \nabla^\alpha$ is the fractal material derivative operator and $\nabla^D \cdot \mathbf{u} = \nabla_x^{\alpha_1} u + \nabla_y^{\alpha_2} v + \nabla_z^{\alpha_3} w$.

If we denote by $\mathbf{a} = \mathbf{a}(a_x, a_y, a_z) = \mathbf{a}(\frac{\partial u}{\partial x}, \frac{\partial v}{\partial y}, \frac{\partial w}{\partial z})$ the vector acceleration of the body subject to the body force $\mathbf{f} = \mathbf{f}(f_x, f_y, f_z)$ acting on the body, then the following fractal momentum and energy equations hold respectively:

$$\rho \frac{\partial u_j}{\partial t} + \rho u_i \nabla_i^{\alpha_i} u_j = \nabla_i^{\alpha_i} \sigma_{ij} + \rho f_j , j = 1, 2, 3 , \tag{5}$$

$$\rho\frac{\partial}{\partial t}\left(\frac{v^2}{2}\right)+\rho u_i\nabla_i^{\alpha_i}\left(\frac{v^2}{2}\right)=u_j\nabla_i^{\alpha_i}\sigma_{ij}+u_j\rho f_j\,,\ j=1,2,3\,, \tag{6}$$

where σ_{ij} is the stress-tensor given by:

$$\sigma_{ij}=-p\delta_{ij}+\mu\left(\nabla_j^{\alpha_j}u_i+\nabla_i^{\alpha_i}u_j\right)+\left(\kappa-\frac{2}{3}\mu\right)\nabla_i^{\alpha_i}u_i\delta_{ij}\,,\ j=1,2,3\,, \tag{7}$$

κ and μ are respectively the bulk and dynamic viscosities, p is the usual thermodynamic pressure and δ_{ij} is the Kronecker delta. Obviously, a linear viscous fluid equation is introduced in equation (7).

If we denote by h the enthalpy of the system which is defined by $h=e+p/\rho$ where e is the internal energy, then using equations (5) and (6), it is easy to verify that the fractal evolution of the enthalpy is given by:

$$\rho\left(\frac{Dh}{Dt}\right)=-\nabla_i^{\alpha_i}(q_i)_{\alpha_i}+\sigma_{ji}\nabla_j^{\alpha_j}u_i+\left(\frac{DP}{Dt}\right)+P\nabla_i^{\alpha_i}u_i\,,\ j=1,2,3\,. \tag{8}$$

Making use of the well-known thermodynamic relations:

$$de=c_v dT-\left(\frac{T\beta_P}{\kappa_T}-p\right)\frac{d\rho}{\rho^2}\,, \tag{9}$$

$$dh=c_p dT+\left(1-T\beta_P\right)\frac{dp}{\rho}\,, \tag{10}$$

where c_v and c_p are respectively the constant volume and pressure heat capacities, $\beta_P=-(1/\rho)(\partial\rho/\partial T)_p$ and $\kappa_T=(1/\rho)(\partial\rho/\partial p)_T$ are respectively the relative changes in density at constant pressure and temperature, it is easy to verify that the following partial differential equations hold:

$$\rho c_p\left(\frac{DT}{Dt}\right)=-\nabla_i^{\alpha_i}(q_i)_{\alpha_i}+\sigma_{ji}\nabla_j^{\alpha_j}u_i+\beta_P T\left(\frac{DP}{Dt}\right)+P\nabla_i^{\alpha_i}u_i\,,\ j=1,2,3\,, \tag{11}$$

$$\rho c_v\frac{DT}{Dt}=-\nabla_i q_i+\sigma_{ji}\nabla_j u_i+\left(\frac{T\beta_P}{\kappa_T}-p\right)\nabla_i^{\alpha_i}u_i\,,\ j=1,2,3\,, \tag{12}$$

$$\frac{\partial}{\partial t}(\rho h)+\nabla_i^{\alpha_i}(\rho u_i h)=-\nabla_i^{\alpha_i}(q_i)_{\alpha_i}+\sigma_{ji}\nabla_j^{\alpha_j}u_i+\left(\frac{DP}{Dt}\right)+P\nabla_i^{\alpha_i}u_i\,,\ j=1,2,3\,, \tag{13}$$

$$c_p\left(\frac{\partial}{\partial t}(\rho T)+\nabla_i^{\alpha_i}(\rho u_i T)\right)=-\nabla_i^{\alpha_i}(q_i)_{\alpha_i}+\sigma_{ji}\nabla_j^{\alpha_j}u_i+\beta_P T\left(\frac{DP}{Dt}\right)+P\nabla_i^{\alpha_i}u_i\,,\ j=1,2,3\,, \tag{14}$$

where $(q_i)_{\alpha_i}=-k\nabla_i^{\alpha_i}T$ is the heat flux [**100,101**], k is a proportionality constant, T is the absolute temperature and

$$\nabla_i^{\alpha_i}(q_i)_{\alpha_i}=-\left(\frac{l_{0i}}{l_i-x_i}\right)^{2\alpha_i-2}\nabla_i\left(k\nabla_i T\right)+\frac{1-\alpha_i}{l_{0i}}\left(\frac{l_{0i}}{l_i-x_i}\right)^{2\alpha_i-1}\nabla_i T\,, \tag{15}$$

where

$$\nabla_i T = \frac{1}{c_p}\nabla_i h - \frac{1-T\beta_P}{\rho c_p}\nabla_i p \ . \tag{16}$$

In order, at the end, to derive the fractal reaction-diffusion equation for the case of an incompressible fluid flow assumed to have a constant density and insignificant pressure, we simply substitute (16) into equation (12) and we use equation (15) which gives at the end:

$$\rho\left(\frac{\partial T}{\partial t} + \left(\mathbf{u}_i \cdot \nabla_i^{\alpha_i}\right)T\right) = k\left(\frac{l_{0i}}{l_i - x_i}\right)^{2\alpha_i - 2}\nabla_i\left(\nabla_i T\right) - \frac{1-\alpha_i}{l_{0i}}\left(\frac{l_{0i}}{l_i - x_i}\right)^{2\alpha_i - 1}\nabla_i T \ . \tag{17}$$

All the previous partial differential equations are reduced to their standard forms for $\alpha_i = 1$. Equation (17) may be interpreted as a scalar form of the fractal bioheat equation with one single variable which will allow us to describe the heat transport in anisotropic materials. This equation generalizes the bioheat equation introduced by Pennes which describes the blood flow in the human body tissues depending on the relative local tissues temperature. The temperature difference between the blood and tissue is taken as a confirmation of its role to eliminate or discharge heat [**102,103**].

By taking into account the metabolic heat generation in the tissue q_m and the contribution of the blood flow to the local tissue temperature distribution q_B , we can use equation (17) to generalize the Pennes bioheat transfer equation to its fractal counterpart:

$$\rho C\frac{\partial T_t}{\partial t} = k_t\left(\left(\frac{l_{0i}}{l_i - x_i}\right)^{2\alpha_i - 2}\nabla_i\left(\nabla_i T_t\right) - \frac{1-\alpha_i}{l_{0i}}\left(\frac{l_{0i}}{l_i - x_i}\right)^{2\alpha_i - 1}\nabla_i T_t\right) + q_B + q_m \ . \tag{18}$$

Here C is the tissue blood specific heat, ρ the tissue density and k_t the tissue thermal conductivity. If one assumes that both the artery and vein maintain a constant temperature when they pass through the tissue region, then the volumetric heat generation rate is given by $q_B = \omega\rho_B C_B (T_B - T_t)$ where ω is the blood perfusion rate, ρ_B is the blood density, C_B is the blood specific heat and T_B is the blood vessel temperature which is assumed to be a constant due to a self-regulation of metabolism. Equation (18) is a partial differential equation for the tissue temperature in fractal dimensions and it can be used under specific and appropriate initial and boundary conditions to derive the transient and steady-state temperature field in the tissue. In this aspect, it should be noted that the temperature of the arterial blood is assumed unaffected in Pennes model when it travels from the heart to the capillary bed, yet, a more realistic model should take into consideration the temperature discrepancy along the artery and the heat evoked by the countercurrent vein [**104**]. The effects of temperature as a critical variable in cancer and experimental immunology are still infrequently considered, yet, some studies prove its importance in the regulation of the immune response and dynamics modulation of the tumor microenvironment [**105,106**]. It is notable that the fractional version of the Pennes bioheat transfer equation which is obtained by replacing the first-time derivative with a derivative of arbitrary positive real order α was discussed in literature through dissimilar arguments [**107,108**].

In the next section, we will analyze the solution of equation (18) and we will discuss its implications in tumor growth. In fact, the solutions of the conventional bioheat equation were discussed largely in literature and their properties are very useful during thermal therapy [**109-111**]. We expect that the fractal solutions will

give rise to some new insights in tumor growth dynamics. In general, one can neglect the metabolic heat generation in the tissue since it is expected to be much slighter than the power density released during hyperthermia treatment [**112-114**]. But this will not affect the solution of the fractal Pennes bioheat transfer equation.

3. Analytical Solution of the Steady-State Fractal Pennes Bioheat Transfer Equation

In order to model the steady-state cell's metabolism and blood perfusion fractal effects on temperature distribution in human bodies, we write equation (18) in one-dimensional spherical coordinates system (axially symmetric system for simplicity) as:

$$\frac{d^2T_t}{dr^2}+\frac{3-\alpha}{r-R}\frac{dT_t}{dr}+\frac{1}{k_t}\left(\omega C_B(T_B-T_t)+q_m\right)\left(\frac{R-r}{R_0}\right)^{2\alpha-2}=0\,. \tag{19}$$

We assume the following boundary conditions known as of 2nd-kind $\frac{dT_t}{dr}(r=R)=0$ and $-k_t\nabla_r T_t(r=R-R_0)=q_m$ which represents heating/cooling by a constant heat flux comparable to the metabolic heat generation in the tissue [**109,115**]. Here R_0 is the radius of the spherical living tissue and R is a characteristic length and may represent the radius of the tumor. In fact, this boundary condition is one of the three types of conditions used on the surface of biological tissue. The further boundary conditions are the 1st-kind which represents the heating/cooling at a constant temperature and the 3rd-kind which represents the heating/cooling by convective heat transfer, i.e. heat exchange between the tissue surface and fluid at a stable temperature. In general, all kinds of boundary conditions may be used to study bioheat transfer in various thermal therapies since they offer information on temperature distribution in biological tissues. For convenience, we introduce the following quantities: $X=R-r$, $A=(\omega C_B T_B+q_m)/R_0^{2\alpha-2}k_t$, $B=\omega C_B/R_0^{2\alpha-2}k_t$ and $Y=A-BT_t$ which simplify equation (19) to:

$$\frac{d^2Y}{dX^2}+\frac{3-\alpha}{X}\frac{dY}{dX}-BX^{2\alpha-2}Y=0\,. \tag{20}$$

The solution of this differential equation is:

$$Y(X)=X^{\frac{\alpha-2}{2}}\left(c_1 I_{\frac{1}{\alpha}-\frac{1}{2}}\left(\frac{\sqrt{B}}{\alpha}X^{\alpha}\right)+c_2 I_{-\frac{1}{\alpha}+\frac{1}{2}}\left(\frac{\sqrt{B}}{\alpha}X^{\alpha}\right)\right), \tag{21}$$

where $c_1, c_2, \ldots$ are constants of integrations and $I_n(x)$ are the modified Bessel function of the 1st-kind. Because of the asymptotic expansions of $I_n(x)$ at $x=0$ which give in our case:

$$I_{\frac{1}{\alpha}-\frac{1}{2}}\left(\frac{\sqrt{B}}{\alpha}X^{\alpha}\right)\approx\left(\frac{\sqrt{B}}{\alpha}\right)^{\frac{1}{\alpha}-\frac{1}{2}}X^{1-\frac{\alpha}{2}}\left(\frac{2^{\frac{1}{2}-\frac{1}{\alpha}}}{\Gamma\left(\frac{1}{2}+\frac{1}{\alpha}\right)}+\frac{2^{-\frac{1}{2}-\frac{1}{\alpha}}B\alpha}{\alpha(\alpha+2)\Gamma\left(\frac{1}{2}+\frac{1}{\alpha}\right)}X^{2\alpha}+\mathrm{O}\left(X^{4\alpha}\right)\right), \tag{22}$$

$$I_{-\frac{1}{\alpha}+\frac{1}{2}}\left(\frac{\sqrt{B}}{\alpha}X^{\alpha}\right)\approx\left(\frac{\sqrt{B}}{\alpha}\right)^{-\frac{1}{\alpha}+\frac{1}{2}}X^{\frac{\alpha}{2}-1}\left(\frac{2^{-\frac{1}{2}+\frac{1}{\alpha}}}{\Gamma\left(\frac{3}{2}-\frac{1}{\alpha}\right)}+\frac{2^{-\frac{3}{2}+\frac{1}{\alpha}}B\alpha}{\alpha(3\alpha-2)\Gamma\left(\frac{3}{2}-\frac{1}{\alpha}\right)}X^{2\alpha}+\mathrm{O}\left(X^{4\alpha}\right)\right), \tag{23}$$

we have $c_2 = 0$. The general solution of equation (19) is therefore given by:

$$T_t(r) = T_B + \frac{q_m}{\omega C_B} - c_1 \left(\frac{R-r}{R_0}\right)^{\frac{\alpha-2}{2}} I_{\frac{1}{\alpha}-\frac{1}{2}}\left(\frac{R_0}{\alpha}\sqrt{\frac{\omega C_B}{k_t}}\left(\frac{R-r}{R_0}\right)^{\alpha}\right). \tag{24}$$

This solution satisfies the boundary condition $\frac{dT_t}{dr}(r=R)=0$ yet the 2nd boundary condition $-k_t \nabla_r T_t(r = R - R_0) = q_m$ gives:

$$c_1 = -\frac{q_m}{k_t\left(\frac{1}{R_0} I_{\frac{1}{\alpha}-\frac{1}{2}}\left(\frac{R_0}{\alpha}\sqrt{\frac{\omega C_B}{k_t}}\right) + \frac{1}{2}\sqrt{\frac{\omega C_B}{k_t}}\left(I_{\frac{1}{\alpha}-\frac{3}{2}}\left(\frac{R_0}{\alpha}\sqrt{\frac{\omega C_B}{k_t}}\right) + I_{\frac{1}{\alpha}+\frac{1}{2}}\left(\frac{R_0}{\alpha}\sqrt{\frac{\omega C_B}{k_t}}\right)\right)\right)}, \tag{25}$$

and at the end, we can write equation (24) as:

$$T_t(r) = T_B + \frac{q_m}{\omega C_B} + \frac{q_m\left(\frac{R-r}{R_0}\right)^{\frac{\alpha-2}{2}} I_{\frac{1}{\alpha}-\frac{1}{2}}\left(\frac{R_0}{\alpha}\sqrt{\frac{\omega C_B}{k_t}}\left(\frac{R-r}{R_0}\right)^{\alpha}\right)}{k_t\left(\frac{1}{R_0} I_{\frac{1}{\alpha}-\frac{1}{2}}\left(\frac{R_0}{\alpha}\sqrt{\frac{\omega C_B}{k_t}}\right) + \frac{1}{2}\sqrt{\frac{\omega C_B}{k_t}}\left(I_{\frac{1}{\alpha}-\frac{3}{2}}\left(\frac{R_0}{\alpha}\sqrt{\frac{\omega C_B}{k_t}}\right) + I_{\frac{1}{\alpha}+\frac{1}{2}}\left(\frac{R_0}{\alpha}\sqrt{\frac{\omega C_B}{k_t}}\right)\right)\right)}. \tag{26}$$

Making use of the following parameter values used in theoretical biology [**116**]: $T_e = 25^0\text{C}$, $T_B = 37^0\text{C}$, $\omega = 3$ Kg/m^{3}s, $C_B = 3850$ J/Kg ^{0}C, $k_t = 0.48$ W/m ^{0}C, $h_H = 8.77$ W/m^2 ^{0}C, $q_m = 1085$ W/m^3 and assuming that the radius of the spherical living cell is $R_0 = 10^{-3}$ m and that the typical radius of the tumor assumed to be a large cell is $R = 2\times 10^{-3}$ m, e.g. lung cancer and lymphoma. [**117,118**], we obtain:

$$T_t(r) \approx 37.0939 + \frac{2260.41\left(\frac{R-r}{R_0}\right)^{\frac{\alpha-2}{2}} I_{\frac{1}{\alpha}-\frac{1}{2}}\left(\frac{155.121R_0}{\alpha}\left(\frac{R-r}{R_0}\right)^{\alpha}\right)}{\frac{1}{R_0} I_{\frac{1}{\alpha}-\frac{1}{2}}\left(\frac{155.121R_0}{\alpha}\right) + 77.56\left(I_{\frac{1}{\alpha}-\frac{3}{2}}\left(\frac{155.121R_0}{\alpha}\right) + I_{\frac{1}{\alpha}+\frac{1}{2}}\left(\frac{155.121R_0}{\alpha}\right)\right)}. \tag{27}$$

This solution shows that the temperature of the living tissue is affected by the fractal dimension. As a first glance, we observe that temperatures are affected by the localization of the tumors and not by the surrounding healthy tissue. We plot in Figures 1-15 the temperature profile $T_t(r)$ in the tumor tissue for different values of α and for different scales after choosing typical values of thermal properties:

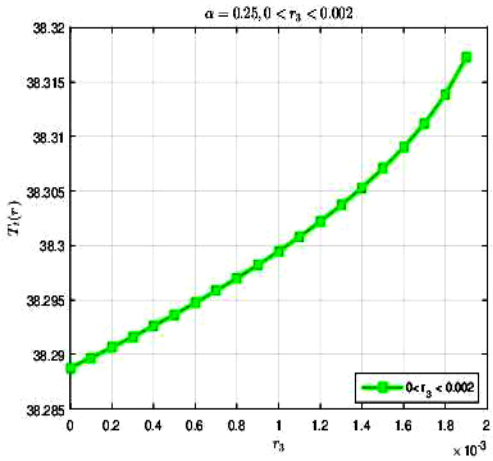

Fig. 1: Variations of $T_t(r)$ for $\alpha = 0.25$ and for $0 < r < 0.002$ m

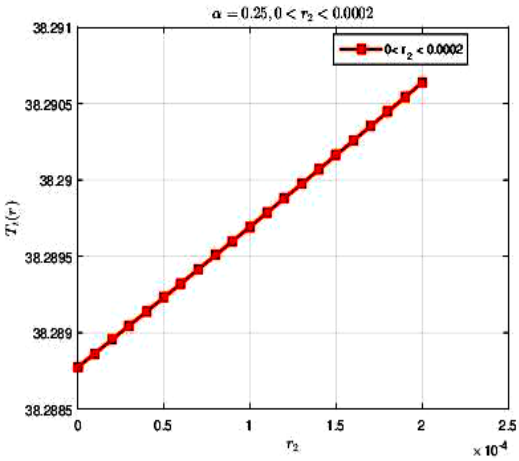

Fig. 2: Variations of $T_t(r)$ for $\alpha = 0.25$ and for $0 < r < 0.0002$ m

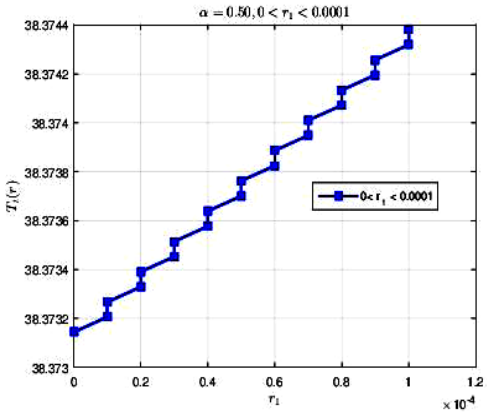

Fig. 3: Variations of $T_t(r)$ for $\alpha = 0.5$ and for $0 < r < 0.0001$ m

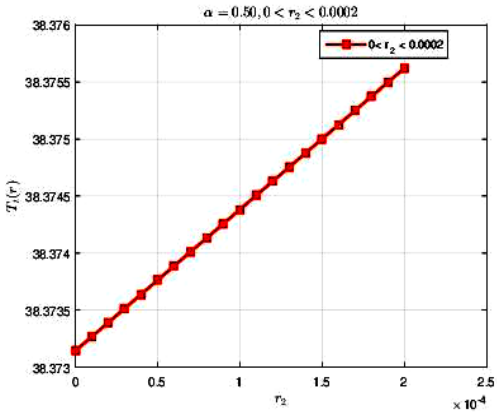

Fig. 4: Variations of $T_t(r)$ for $\alpha = 0.5$ and for $0 < r < 0.0002$ m

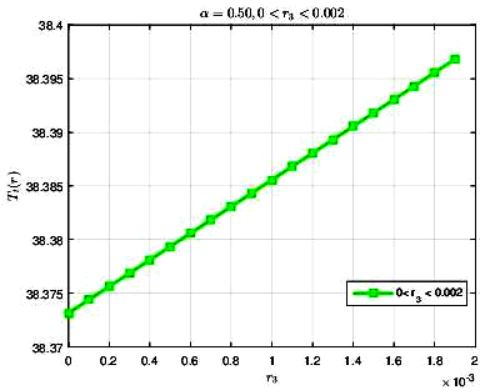

Fig. 5: Variations of $T_t(r)$ for $\alpha = 0.5$ and for $0 < r < 0.002$ m

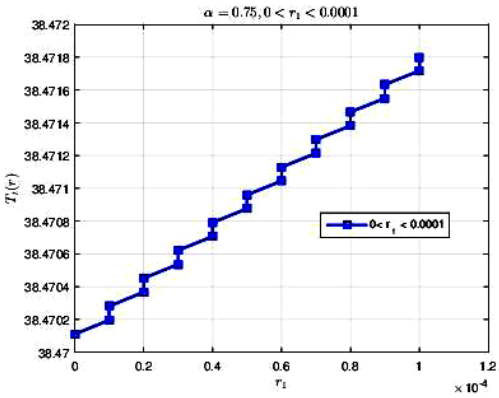

Fig. 6: Variations of $T_t(r)$ for $\alpha = 0.75$ and for $0 < r < 0.0001$ m

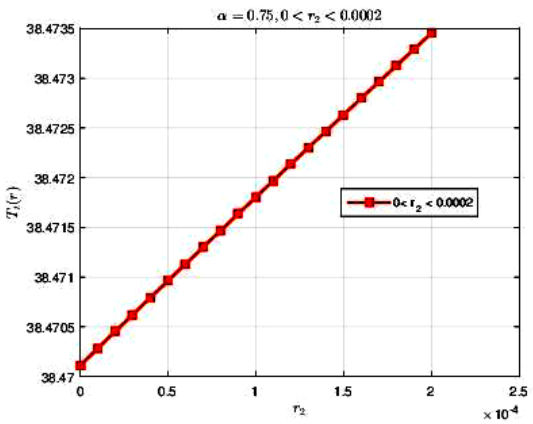

Fig. 8: Variations of $T_t(r)$ for $\alpha = 0.75$ and for $0 < r < 0.0002$ m

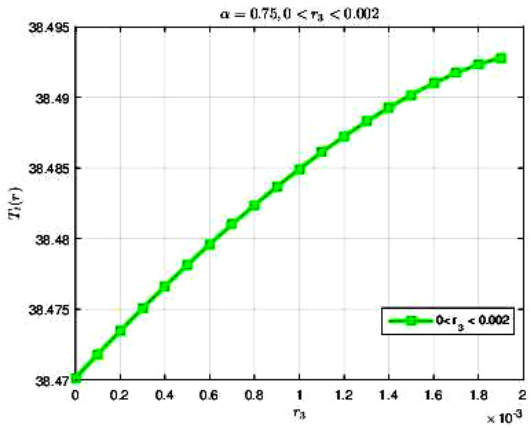

Fig. 9: Variations of $T_t(r)$ for $\alpha = 0.75$ and for $0 < r < 0.002$ m

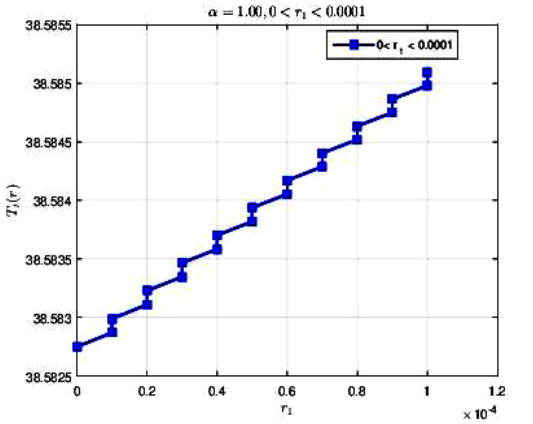

Fig. 10: Variations of $T_t(r)$ for $\alpha = 1$ and for $0 < r < 0.0001$ m

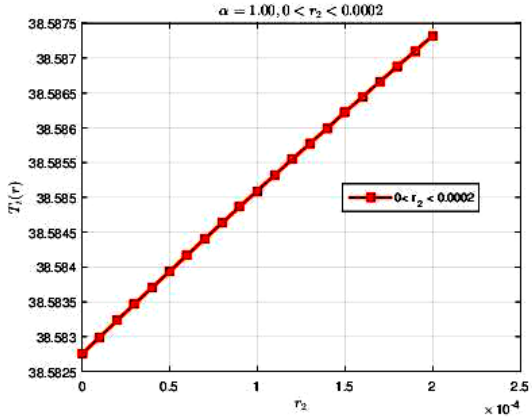

Fig. 11: Variations of $T_t(r)$ for $\alpha = 1$ and for $0 < r < 0.0002$ m

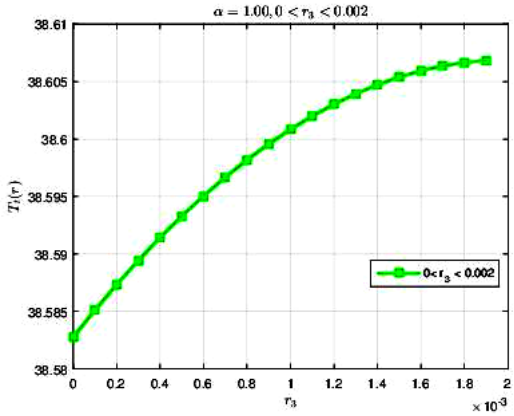

Fig. 12: Variations of $T_t(r)$ for $\alpha = 1$ and for $0 < r < 0.002$ m

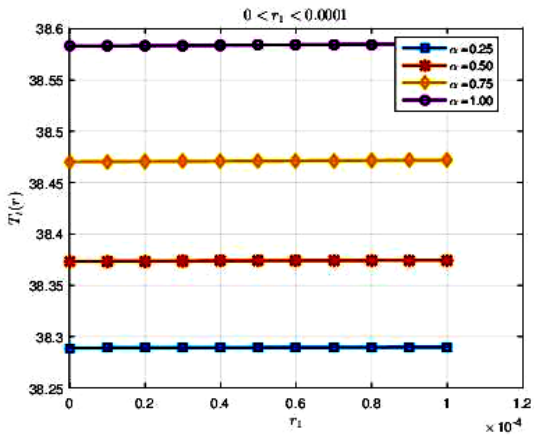

Fig. 13: Comparing the variations of $T_t(r)$ for different values of α and for $0 < r < 0.0001$ m

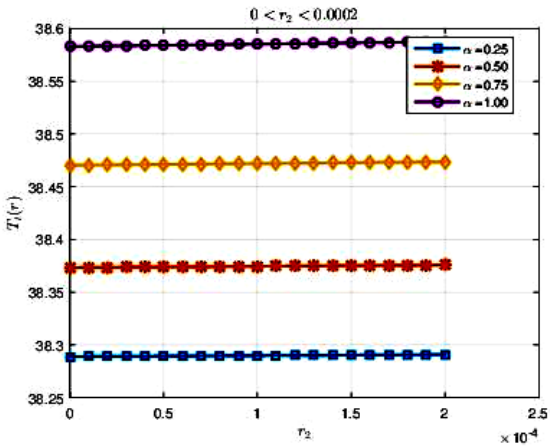

Fig. 14: Comparing the variations of $T_t(r)$ for different values of α and for $0 < r < 0.0002$ m

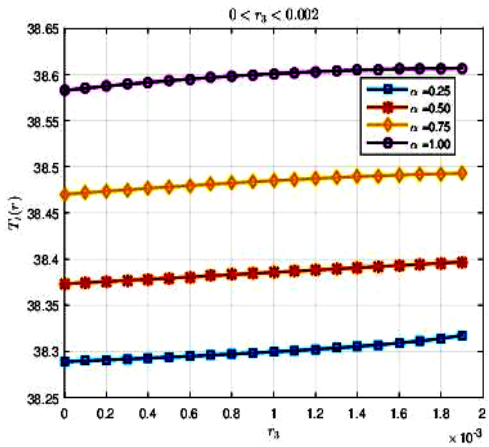

Fig. 15: Comparing the variations of $T_t(r)$ for different values of α and for $0 < r < 0.002$ m

We observe from Figures 1-12 that the temperature increases with the radial distance and the difference between the minimum and the maximum temperature is not too large. Yet, the problem is sensitive to the numerical values of α and the range of r as it is shown in Figures 13-15. The larger the value of α, the enhanced is the temperature. The range of the temperature lies between $38.28^{\circ}\mathrm{C}$ and $38.58^{\circ}\mathrm{C}$, hence the response temperature is larger than $37^{\circ}\mathrm{C}$. We also observe in some cases such as Figures 3, 6 and 10 that the temperature increases in a quasi-oscillating way with the radial distance. The response temperature corresponding to the quasi-oscillating solution is maintained larger than the input temperature of the human body or the arterial blood. The effects of fractal dimensions and length tissues scales are related to the quasi-oscillation of the tissue temperature, although the mean temperature is almost the same for some particular cases. These solutions reveal the oscillations of the temperature inside the tissue over time which are affected by fractal dimensions. In other words, these results show that, besides the effect of thermal conductivity of tissue and blood perfusion rate, fractal dimensions affect the tissue temperature. These solutions are practical to determine the required temperature to kill the malignant cells as well as optimizing the treatment procedure.

The tumor surface temperature is not constant and varies in a certain range of temperature depending on the value of α and the rage of r. However, we observed that the range of $0 < \alpha \le \frac{1}{2}$ keeps the temperature of the body lower than $38.3^{\circ}\mathrm{C}$. These analytical and numerical solutions can provide good information of fractal thermal behavior of living tissues [**119,120**]. Undoubtedly, in the present model, the human body and tumor are assumed to be consistent media with averaged physical parameters, therefore the numerical graphs are somewhat dissimilar from those obtained in real-world applications during hyperthermia treatment. It was observed that when tumor-bearing mice are subject to temperatures between $39^{\circ}\mathrm{C}$ and $43^{\circ}\mathrm{C}$, there is an increase in tumor oxygenation up to one-day hours after heating. There is a correlation between the level of reoxygenation and the radiation sensitivity of the tumor as observed in studies with canine sarcomas and in clinical trials of patients with soft tissue sarcomas and breast cancer [**115,121,122**]. It is noteworthy that at very high temperature, if cells are kept at a temperature between $42^{\circ}\mathrm{C}$ and $45^{\circ}\mathrm{C}$, then proteins will be destroyed and, hence, cells will decease [**111**]. It is noteworthy at the end that the oscillations of body temperature may give an insight into control of breathing and the cardiovascular system [**123**].

We can evaluate the heat conduction from equation (27) using the relation $(q)_\alpha(r) = -k_t \nabla^\alpha T$ which gives:

$$(q)_\alpha(r) = \frac{1095Q(r)}{\frac{1}{R_0} I_{\frac{1}{\alpha}-\frac{1}{2}}\left(\frac{155.121R_0}{\alpha}\right) + 77.56\left(I_{\frac{1}{\alpha}-\frac{3}{2}}\left(\frac{155.121R_0}{\alpha}\right) + I_{\frac{1}{\alpha}+\frac{1}{2}}\left(\frac{155.121R_0}{\alpha}\right)\right)}, \quad (28)$$

where

$$Q(r) = \frac{1}{R_0}\frac{\alpha-2}{2}\left(\frac{R-r}{R_0}\right)^{-\left(\frac{2+\alpha}{2}\right)} I_{\frac{1}{\alpha}-\frac{1}{2}}\left(\frac{155.121R_0}{\alpha}\left(\frac{R-r}{R_0}\right)^{\alpha}\right)$$

$$+\left(\frac{R-r}{R_0}\right)^{\frac{\alpha-2}{2}}\left(77.56\left(I_{\frac{1}{\alpha}-\frac{3}{2}}\left(\frac{155.121R_0}{\alpha}\left(\frac{R-r}{R_0}\right)^{\alpha}\right) + I_{\frac{1}{\alpha}+\frac{1}{2}}\left(\frac{155.121R_0}{\alpha}\left(\frac{R-r}{R_0}\right)^{\alpha}\right)\right)\right). \quad (29)$$

The volumetric heat generation rate is given by $q_B = \omega\rho_B C_B (T_B - T_t)$ and for a blood density $\rho_B \approx 1060\ \mathrm{Kg}\times\mathrm{m}^{-3}$, we can estimate the variations of q_B with respect to the position of the tumor growth using equation (27). We plot in Figures 16-30 the variations of the regional heat source $Q(r)$ for two different values of α:

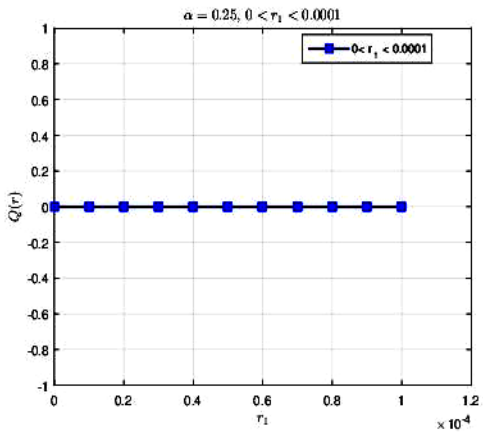

Fig. 16: Variations of $Q(r)$ for $\alpha = 0.25$ and for $0 < r < 0.0001$ m

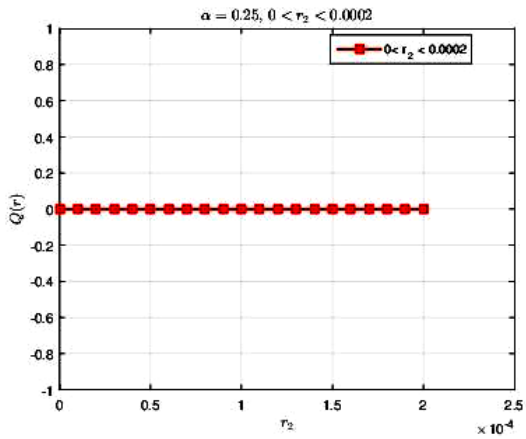

Fig. 17: Variations of $Q(r)$ for $\alpha = 0.25$ and for $0 < r < 0.0002$ m

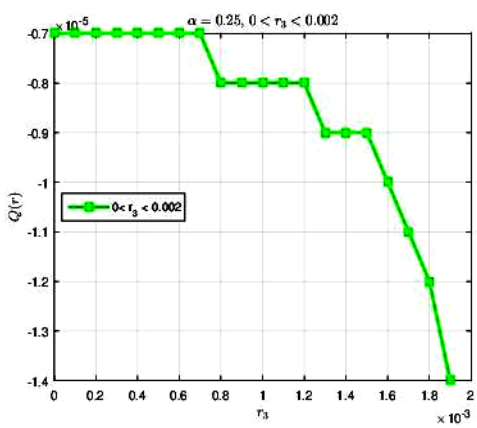

Fig. 18: Variations of $Q(r)$ for $\alpha = 0.25$ and for $0 < r < 0.002$ m

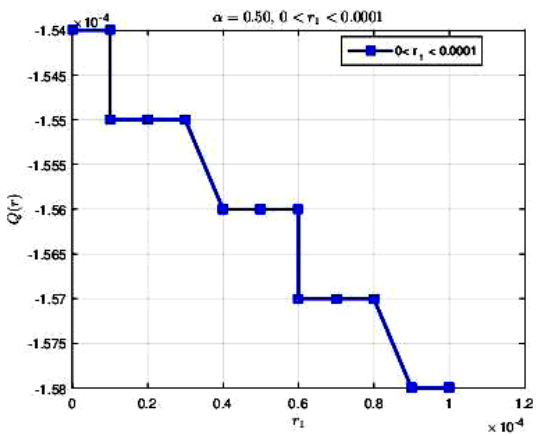

Fig. 19: Variations of $Q(r)$ for $\alpha = 0.5$ and for $0 < r < 0.0001$ m

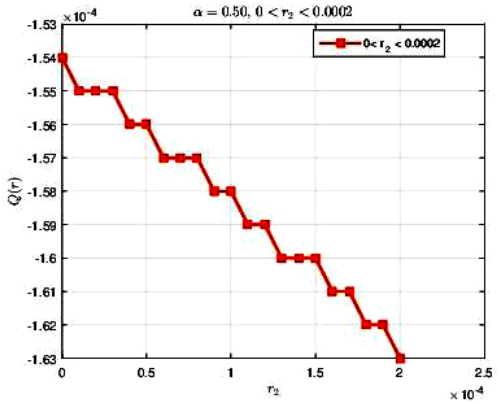

Fig. 20: Variations of $Q(r)$ for $\alpha = 0.5$ and for $0 < r < 0.0002$ m

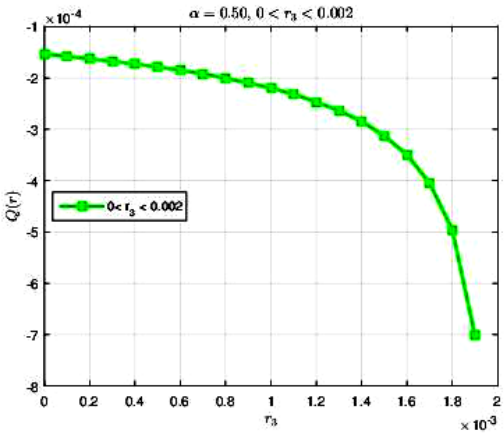

Fig. 21: Variations of $Q(r)$ for $\alpha = 0.5$ and for $0 < r < 0.002$ m

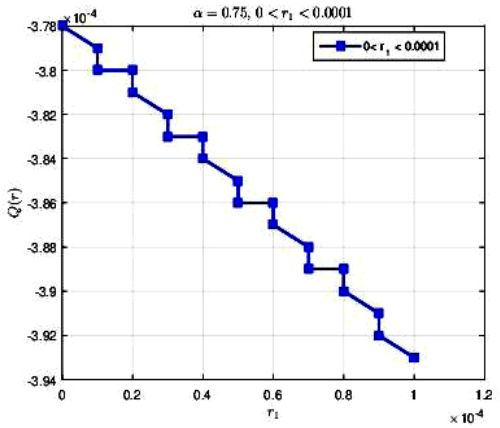

Fig. 23: Variations of $Q(r)$ for $\alpha = 0.75$ and for $0 < r < 0.0001$ m

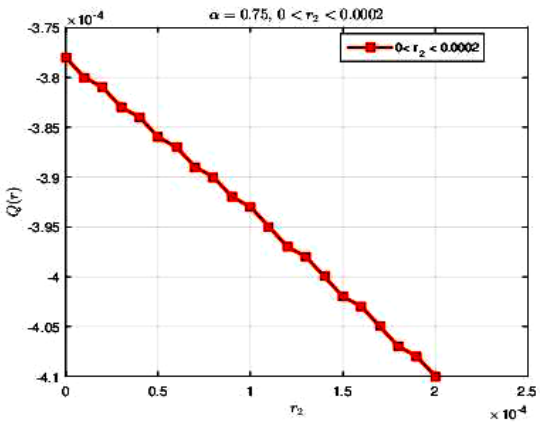

Fig. 24: Variations of $Q(r)$ for $\alpha = 0.75$ and for $0 < r < 0.0002$ m

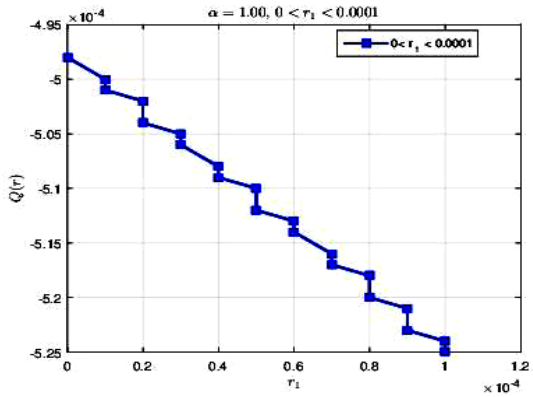

Fig. 25: Variations of $Q(r)$ for $\alpha = 1$ and for $0 < r < 0.0001$ m

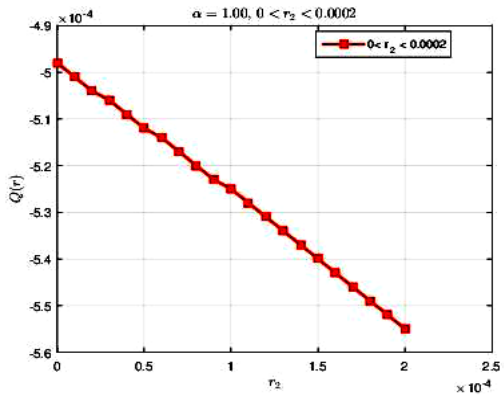

Fig. 26: Variations of $Q(r)$ for $\alpha = 1$ and for $0 < r < 0.0002$ m

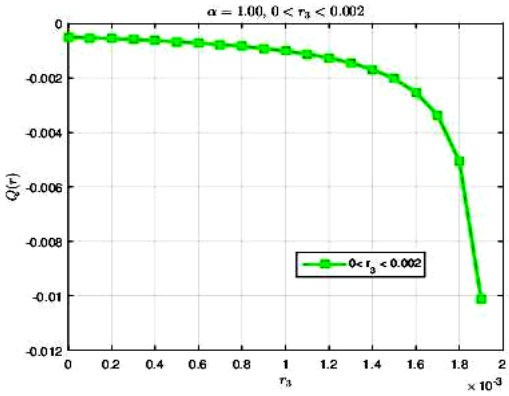

Fig. 27: Variations of $Q(r)$ for $\alpha = 1$ and for $0 < r < 0.002$ m

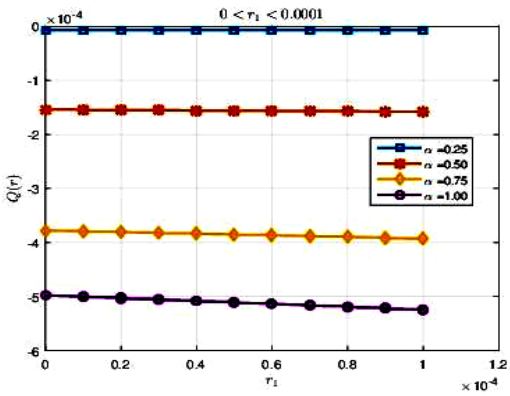

Fig. 28: Comparing the variations of $Q(r)$ for different values of α and for $0 < r < 0.0001$ m

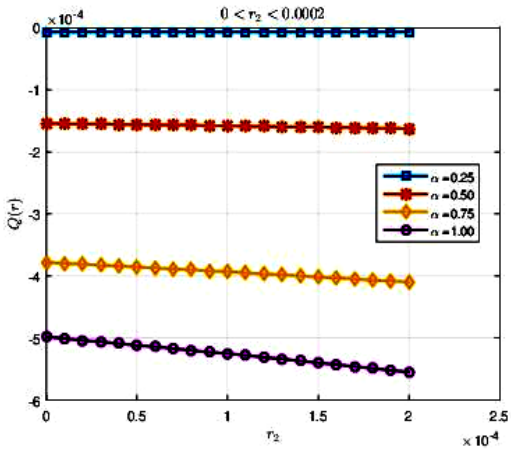

Fig. 29: Comparing the variations of $Q(r)$ for different values of α and for $0 < r < 0.0002$ m

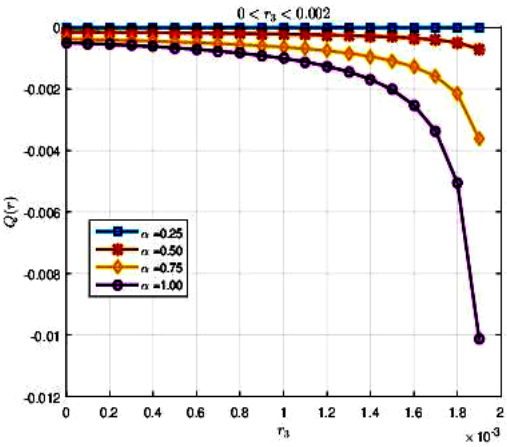

Fig. 30: Comparing the variations of $Q(r)$ for different values of α and for $0 < r < 0.002$ m

We observe again that the value of $0 < \alpha \leq \frac{1}{2}$ leads to negligible variations of $Q(r)$ as it is shown in Figures 28, 29 and 30. Whereas for $\frac{1}{2} \leq \alpha < 1$, $Q(r)$ starts to decrease toward negative values and the heat conduction lies in the negative region. This shows that heat flux in the presence of a tumor growth moves from higher temperature regions to lower temperature regions. In particular cases as shown in Figures 18, 19, 20, 23, 24 and 25, the variations of $Q(r)$ are quasi-oscillating. In general, in all living systems, the oscillations of heat flux and heat flow are driven by certain biochemical processes, e.g. phosphorylation and dephosphorylation reactions catalyzed by the cell-cycle oscillator [**124**]. This may have important impacts on the thermodynamic process of living cells. Understanding the underlying oscillatory phenomena is important in medicine in order to improve current methods and to develop new techniques including heat transfer at nanoscale levels which will allow to better study cell tissues and their viability and biological properties [**125**].

4. Analytical Solution of the Time-Dependent Fractal Pennes Bioheat Transfer Equation

In this section, we concentrate ourselves to the temperature distribution in tumor tissue based on the non steady-state bioheat transfer in the cell tissue in the presence of the tumor growth. We start by solving equation (18) which may be written as:

$$\frac{\rho C_B}{k_t}\frac{\partial T_t}{\partial t}=\left(\frac{R-r}{R_0}\right)^{2-2\alpha}\left(\frac{\partial^2 T_t}{\partial r^2}+\frac{3-\alpha}{r-R}\frac{\partial T_t}{\partial r}\right)+\frac{\omega C_B T_B+q_m}{k_t}-\frac{\omega C_B}{k_t}T_t\ ,$$

$$\equiv\left(\frac{R-r}{R_0}\right)^{2-2\alpha}\left(\frac{\partial^2 T_t}{\partial r^2}+\frac{3-\alpha}{r-R}\frac{\partial T_t}{\partial r}\right)+\bar{A}-\bar{B}T_t\ , \tag{30}$$

where $\bar{A}=(\omega C_B T_B+q_m)/k_t$ and $\bar{B}=\omega C_B/k_t$. By letting $Q(r,t)=\bar{A}-\bar{B}T_t(r,t)$, we can write equation (30) as:

$$\frac{\rho C_B}{k_t}\frac{\partial Q}{\partial t}=\left(\frac{R-r}{R_0}\right)^{2-2\alpha}\left(\frac{\partial^2 Q}{\partial r^2}+\frac{3-\alpha}{r-R}\frac{\partial Q}{\partial r}\right)-BQ\ . \tag{31}$$

We can use the separation of variables method by letting $Q(r,t)=F(t)G(r)$ which splits equation (31) into the following differential equations:

$$\frac{\partial^2 G}{\partial r^2}+\frac{3-\alpha}{r-R}\frac{\partial G}{\partial r}-\left(\frac{\omega C_B}{k_t}-\lambda^2\right)\left(\frac{R-r}{R_0}\right)^{2\alpha-2}G=0\ , \tag{32}$$

and

$$\frac{\partial F}{\partial t}+\frac{\lambda^2 k_t}{\rho C_B}F=0\ . \tag{33}$$

λ^2 is here a separation of variable. The solution of equation (33) is given by $F=F_0 e^{-k_t\lambda^2 t/\rho C_B}$ with $F_0=F(t=0)$ whereas the solution of equation (32) is given by:

$$G(r)=c_3\left(R-r\right)^{\frac{\alpha-2}{2}}I_{\frac{1}{\alpha}-\frac{1}{2}}\left(\frac{R_0}{\alpha}\sqrt{\frac{\omega C_B}{k_t}-\lambda^2}\left(\frac{R-r}{R_0}\right)^{\alpha}\right). \tag{34}$$

The general solution using the boundary condition $\frac{dG}{dr}(r=R)=0$ and $-k_t\nabla_r G(r=R-R_0)=q_m$ gives:

$$T_t(r,t)=T_B+\frac{q_m}{\omega C_B}+\frac{F_0 q_m e^{-k_t\lambda^2 t/\rho C_B}\left(\frac{R-r}{R_0}\right)^{\frac{\alpha-2}{2}}I_{\frac{1}{\alpha}-\frac{1}{2}}\left(\frac{R_0}{\alpha}\sqrt{\frac{\omega C_B}{k_t}-\lambda^2}\left(\frac{R-r}{R_0}\right)^{\alpha}\right)}{k_t\left(\frac{1}{R_0}I_{\frac{1}{\alpha}-\frac{1}{2}}\left(\frac{R_0}{\alpha}\sqrt{\frac{\omega C_B}{k_t}-\lambda^2}\right)+\frac{1}{2}\sqrt{\frac{\omega C_B}{k_t}}\left(I_{\frac{1}{\alpha}-\frac{3}{2}}\left(\frac{R_0}{\alpha}\sqrt{\frac{\omega C_B}{k_t}-\lambda^2}\right)+I_{\frac{1}{\alpha}+\frac{1}{2}}\left(\frac{R_0}{\alpha}\sqrt{\frac{\omega C_B}{k_t}-\lambda^2}\right)\right)\right)}\ . \tag{35}$$

For very large time, it is observed that $T_t(r,t)\to T_B+q_m/\omega C_B\approx 37.10^{\circ}\mathrm{C}$ which corresponds to a slight elevation in temperature. We plot in figures 31-35 the 3D variations of the temperature for different values of α and for different scales for an average tissue density of $\rho\approx 1100\ \mathrm{Kg}\times\mathrm{m}^{-3}$ $F_0=F(t=0)=1$ and $\lambda^2=1$:

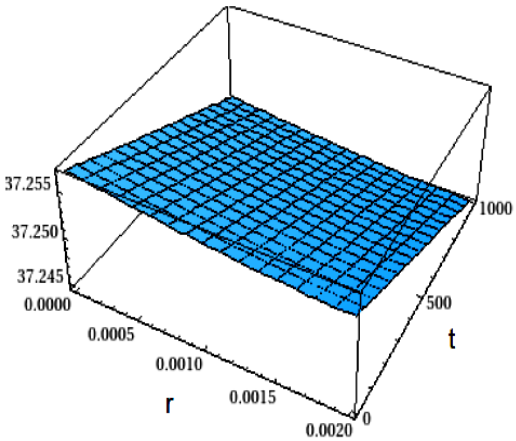

Fig.31: Plot of $T_t(r,t)$ for $\alpha = 0.75$

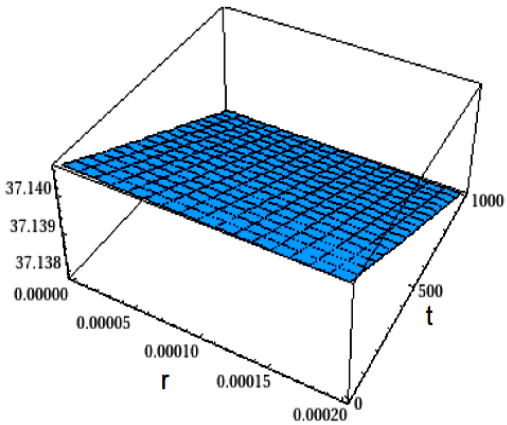

Fig.32: Plot of $T_t(r,t)$ for $\alpha = 0.5$

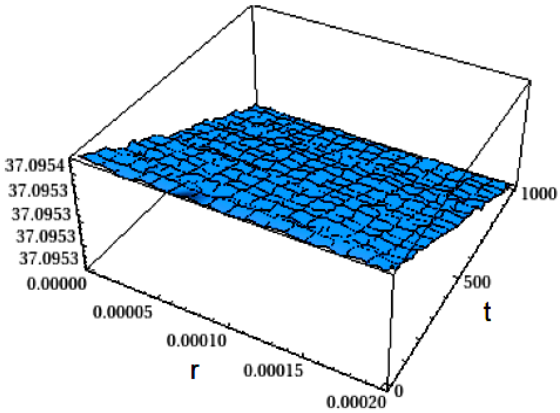

Fig.33: Plot of $T_t(r,t)$ for $\alpha = 25$

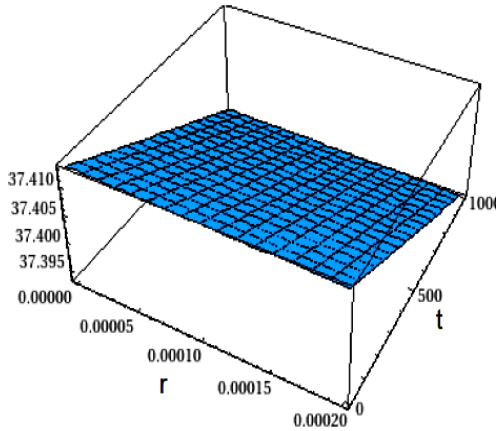

Fig.34: Plot of $T_t(r,t)$ for $\alpha = 0.25$ and for $0 < r < 0.0002$ m

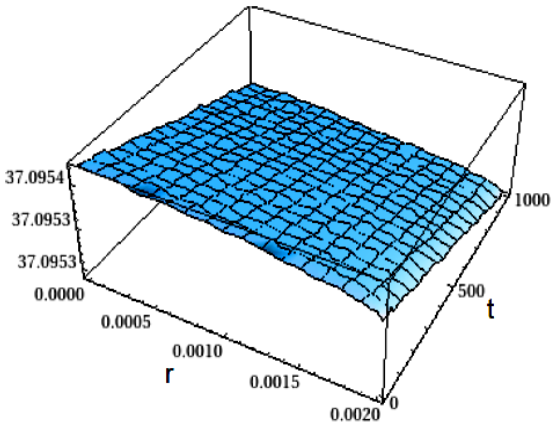

Fig.35: Plot of $T_t(r,t)$ for $\alpha = 0.25$ and for $0 < r < 0.002$ m

We observe that the variations of the temperature in the presence of a tumor growth are affected by fractal dimensions and the scales used even though the variations are slightly comparable. The temperature is subject to a decreasing state in the presence of the tumor growth. For $0 < \alpha < \frac{1}{2}$, the temperature is decreasing but is subject to small fluctuations with time as it is obvious from Figures 33 and 35 for two different length scales.

These are roughly estimates of the variations of temperature, yet several constraints must be used to obtain accurate data. Nevertheless, these results prove that fractal dimensions, the radius of the tumor growth and the dimension of the living cell tissue are all important parameters in bioheat transfer analysis. Undeniably, in the case of a moderately shallow tumour a boundary condition modelling the skin-environment interface is required to solve the fractal Pennes bioheat equation. Nevertheless, LOSA provides an effective means for solving fractal bio-heat transfer in soft biological tissue and may be suited for real-time applications.

The previous approach may be extended to study the fractal thermal wave model of Pennes bioheat equation since in general the biological tissues are the materials with non-homogeneous inner structure and hence the Cattaneo-Vernotte hyperbolic heat equation (CVHEH) should be used [**126,127**]. This equation was explored in literature through dissimilar frameworks [**128-131**]. The simplest form of the fractal CVHEH is:

$$\tau\frac{\partial^2 T_t}{\partial t^2}+\left(1+\frac{\tau k_t}{C_B}\right)\frac{\partial T_t}{\partial t}=\tau v^2\left(\left(\frac{l_{0i}}{l_i-x_i}\right)^{2\alpha_i-2}\nabla_i\left(\nabla_i T_t\right)-\frac{1-\alpha_i}{l_{0i}}\left(\frac{l_{0i}}{l_i-x_i}\right)^{2\alpha_i-1}\nabla_i T_t\right)+\frac{k_t}{C_B}\left(T_B-T_t\right)+\frac{q_m}{C_B},\quad(36)$$

where τ is the relaxation time, $v=\sqrt{a/\tau}$ is the velocity of the thermal wave with a being the thermal diffusivity. This equation may be written as:

$$\tau\frac{\partial^2 T_t}{\partial t^2}+\left(1+\frac{\tau k_t}{C_B}\right)\frac{\partial T_t}{\partial t}=\tau v^2\left(\frac{R-r}{R_0}\right)^{2-2\alpha}\left(\frac{\partial^2 T_t}{\partial r^2}+\frac{3-\alpha}{r-R}\frac{\partial T_t}{\partial r}\right)+\frac{k_t T_B+q_m}{C_B}-\frac{k_t}{C_B}T_t\,,\quad(37)$$

and its solution is obtained by letting $P(r,t)=E-UT_t(r,t)$ where $E=(k_tT_B+q_m)/C_B$ and $U=k_t/C_B$. This converts easily equation (37) to:

$$\tau\frac{\partial^2 P}{\partial t^2}+\left(1+\frac{\tau k_t}{C_B}\right)\frac{\partial P}{\partial t}=\tau v^2\left(\frac{R-r}{R_0}\right)^{2-2\alpha}\left(\frac{\partial^2 P}{\partial r^2}+\frac{3-\alpha}{r-R}\frac{\partial P}{\partial r}\right)-UP\,.\quad(38)$$

The separation of variables method $P(r,t)=H(t)K(r)$ splits equation (38) into the following differential equations:

$$\frac{\partial^2 K}{\partial r^2}+\frac{3-\alpha}{r-R}\frac{\partial K}{\partial r}-\frac{U-\eta^2}{\tau v^2}\left(\frac{R-r}{R_0}\right)^{2\alpha-2}K=0\,,\quad(39)$$

and

$$\tau\frac{\partial^2 H}{\partial t^2}+\left(1+\frac{\tau k_t}{C_B}\right)\frac{\partial H}{\partial t}+\eta^2 H=0\,,\quad(40)$$

η^2 is another separation of variable. It is easy to verify that the general solution is given by:

$$T_t(r,t)=\frac{k_tT_B+q_m}{C_B}+K\frac{C_B}{k_t}e^{-\frac{1}{2\tau}\left(\sqrt{\left(1+\frac{\tau k_t}{C_B}\right)^2-4\tau\eta^2}+1+\frac{\tau k_t}{C_B}\right)t}\left(\frac{R-r}{R_0}\right)^{\frac{\alpha-2}{2}}I_{\frac{1}{\alpha}-\frac{1}{2}}\left(\frac{R_0}{\alpha}\sqrt{\frac{U-\eta^2}{\tau v^2}}\left(\frac{R-r}{R_0}\right)^{\alpha}\right),\quad(41)$$

where K is a constant of integration which may be derived from suitable boundary conditions. We plot in the Figures 36-39 the variations of $T_t(r,t)$ for different scales ranges after fixing the relaxation time to $\tau=10$ s and evaluating the integration constant for fixed parameters values used in theoretical biology [**116**]:

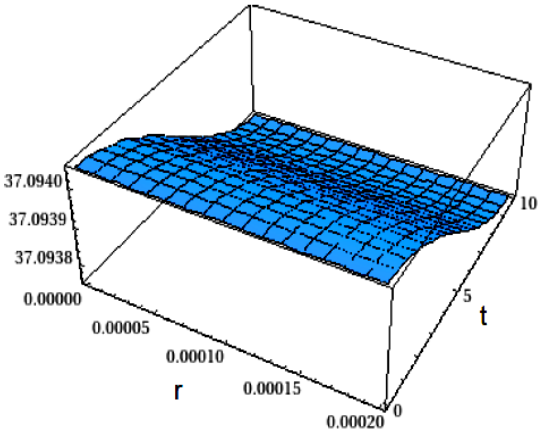

Fig.36: Plot of $T_t(r,t)$ for $\alpha = 0.75$

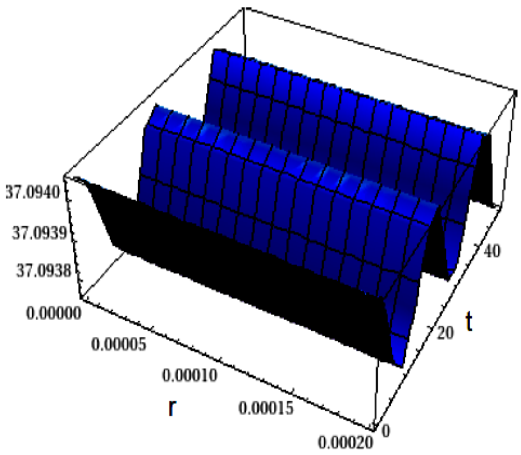

Fig.37: Plot of $T_t(r,t)$ for $\alpha = 0.75$ for large range of time

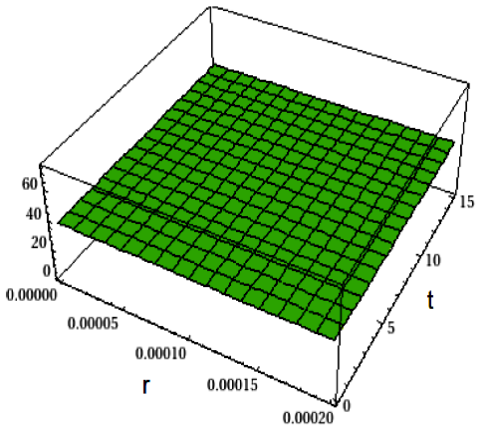

Fig.38: Plot of $T_t(r,t)$ for $\alpha = 0.25$

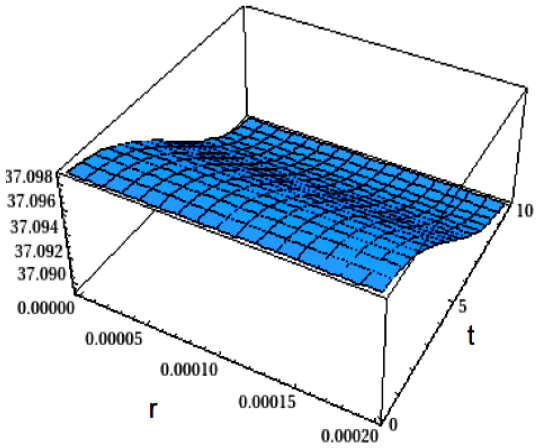

Fig.39: Plot of $T_t(r,t)$ for $\alpha = 1$

These plots illustrate the decaying behavior of $T_t(r,t)$. The analytical solution can predict therefore the decaying temperature in the living tissue for small range of time and its oscillatory behavior for large range of time. This result is in agreement with several medical studies [**132,133**]. The amplitude of oscillations is not altered for large period of time and the temperature of living tissue oscillates between $38^\circ\mathrm{C}$ and $37^\circ\mathrm{C}$ in the presence of the tumor growth for $\frac{1}{2} < \alpha < 1$ whereas the range of the temperature oscillations is within $37^\circ\mathrm{C}$ for low length scales. The case $\alpha = \frac{1}{2}$ leads to a steady-state temperature as it is obvious from Figure 38.

One may extend the LOSA by replacing $c_1^{(k)}$ by:

$$c_{12}^{(k)} = \left(\frac{r - R_1}{R_{01}}\right)^{\alpha-1} + \left(\frac{R_2 - r}{R_{02}}\right)^{\alpha-1}, r \in (R_1, R_2), \tag{42}$$

with R_{01} and R_{02} are characteristic lengths [**134**]. This generalization may be used to differentiate between two fractal media having the same fractal dimension but different density distributions, e.g. localization of two tumors growths. In that case, $\frac{\partial}{\partial r} := \nabla_r \to \nabla_r^{\alpha} = c_{12}^{-(k)}\nabla$ and the fractal bioheat equation takes the following form:

$$\rho C\frac{\partial T_t}{\partial t}=k_t\frac{1}{\left(\left(\frac{r-R_1}{R_{01}}\right)^{\alpha-1}+\left(\frac{R_2-r}{R_{02}}\right)^{\alpha-1}\right)^2}\left(\Delta T_t-(\alpha-1)\frac{\frac{1}{R_{01}}\left(\frac{r-R_1}{R_{01}}\right)^{\alpha-2}-\frac{1}{R_{02}}\left(\frac{R_2-r}{R_{02}}\right)^{\alpha-2}}{\left(\frac{r-R_1}{R_{01}}\right)^{\alpha-1}+\left(\frac{R_2-r}{R_{02}}\right)^{\alpha-1}}\nabla T_t\right)+q_B+q_m\,. \quad (43)$$

The steady-state Pennes fractal equation takes then the form:

$$\Delta T_t-(\alpha-1)\frac{\frac{1}{R_{01}}\left(\frac{r-R_1}{R_{01}}\right)^{\alpha-2}-\frac{1}{R_{02}}\left(\frac{R_2-r}{R_{02}}\right)^{\alpha-2}}{\left(\frac{r-R_1}{R_{01}}\right)^{\alpha-1}+\left(\frac{R_2-r}{R_{02}}\right)^{\alpha-1}}\nabla T_t+\frac{1}{k_t}\left(\left(\frac{r-R_1}{R_{01}}\right)^{\alpha-1}+\left(\frac{R_2-r}{R_{02}}\right)^{\alpha-1}\right)^2\left(q_B+q_m\right)=0\,. \quad (44)$$

Following the arguments of [**135**], this generalization is practical to study heat dissipative processes, e.g. heat dissipation by the blood flow besides others biological effects [**136-140**]. This will be analyzed in a future work.

5. Conclusions and Perspectives

In this study, we have discussed the implications of the concept of the "product-like fractal measure" introduced by Li and Ostoja-Starzewski (LOSA) in bioheat transfer theory which is widely used in medicine, in particular thermal treatments of cancer. This approach is in fact characterized by fractal dimensions and a modified gradient operator which depends on a length R representing the radius of the tumor and another length R_0 representing the spherical living tissue radius. Such a methodology is new and was not discussed to the best of our knowledge in literature. Throughout this study, we have assumed that the typical radius of the tumor is large.

The fractal kinetic equations lead to a fractal formulation of the Pennes bioheat transfer equation. The solution of one-dimensional steady-state fractal Pennes bioheat transfer equation has been solved, and the corresponding equation has been solved analytically and numerically. The analytical solutions have been explored after taking into account the boundary conditions of 2nd-kind. We have discussed both the steady and unsteady equations and we have derive their corresponding solutions after assuming a specific heating/cooling with a constant heat flux analogous to the metabolic heat generation in the tissue. In both cases, it was observed that the solutions, i.e. the response temperatures are affected by fractal dimensions, the radius of the tumor growth and the dimension of the living cell tissue. Our study confirms that realistic estimates of the temperature and fractal thermal behavior of living tissues are affected by the numerical value of α. The quasi-oscillations of the heat flux obtained throughout this study may have also an effect on body temperature and vice versa and confirm theoretically predicted results. So, we can say that fractal dimensions play a crucial role in understanding of thermal and biomechanical properties of human tissues and physics that governs biological processes. The accuracy of fractal thermal modeling of human tissue greatly depends on the numerical value of α.

We have also discussed the Cattaneo-Vernotte hyperbolic heat equation. The solutions obtained indicate the presence of a decaying temperature for small length scales and short period of time and oscillatory variations

for small length scales and long period of time. These give rise to an oscillating heat flux with constant amplitude which is affected by the value of the relaxation time, the numerical value of the fractal dimension, the radius of the tumor growth and the dimension of the living cell tissue. The amplitude of oscillations is not altered for large period of time: in particular, for $\frac{1}{2} < \alpha < 1$, the temperature of living tissues in the presence of a tumor growth decreases with time till it reaches the temperature of around $37^{\circ}\mathrm{C}$. For $0 < \alpha < \frac{1}{2}$, as steady state solution is obtained.

The clinical application of LOSA could be demonstrated using an assortment of modalities for thermal treatment. We know that thermal therapy uses dissimilar energy sources to produce heat in order to cause thermal damage to choosy targets such as tumors/cancers. This is achieved by having good information about tissues temperatures for tumor treatment in order not to destroy the nearby tissue when using adequate thermal energy.

We conclude that, LOSA in general, holds motivating features and may play an important role in controlling temperature distribution in living tissue in the presence of tumor growth. It will be of interest to extend this work for different boundary conditions, e.g. sinusoidal heat flux boundary condition which are practical at the skin surface. It is also inspiring to extend our approach by implementing nonlocal effects which are important for biological and medical systems where numerous cells effects may exist on the cellular level. Moreover, it will of interest to extend LOSA to study the fractal heat propagation equations in tissue to optimize outcomes of thermal ablative treatments and to analyze the corresponding quantitative results. These will be the main goals of our future work.

Disclosure of Conflicts of Interest: The author declares that they have no known competing financial interests or personal relationships that could have appeared to influence the work reported in this paper.
Funding: The author would like to thank Chiang Mai University for funding this research.
Data availability statement: The author confirms the absence of sharing data.
Acknowledgments: The author would like to thank the group of anonymous referees for their useful comments and valuable suggestions.

REFERENCES

[1] P. L. Krapivsky, S. Redner, E. Ben-Naim, A Kinetic View of Statistical Physics, Cambridge University Press, Cambridge, 2010.
[2] K. J. Falconer, Fractal Geometry-Mathematical Foundations and Applications, Wiley, New York, 2003.
[3] B. B. Mandelbrot, The Fractal Geometry of Nature, W. H. Freeman and Company, New York, 1983.
[4] B. A. Snopok, Nonexponential kinetics of surface chemical reactions, Theor. Exp. Chem. 50, (2014) 67-95.
[5] K. J. Ellis, Neutron and Muon Studies of Spin Dynamics in Magnetic Systems. Diss. University of Huddersfield, Huddersfield, 2013.
[6] A. W. Marczewski, A. Deryło-Marczewska, A. Słota, Adsorption and desorption kinetics of benzene derivatives on mesoporous carbons, Adsorption 19, (2013) 391-406.
[7] H. Li, S. Chen, H. Zhao, Fractal mechanisms for the allosteric effects of proteins and enzymes, Biophys. J. 58, (1990) 1313-1320.
[8] R. Kopelman, Rate processes on fractal: theory, simulations, and experiments, J. Stat. Phys. 42, (1986) 185-200.
[9] K. Lindenberg, W. S. Sheu, R. Kopelman, Scaling properties of diffusion-limited reactions on fractal and Euclidean geometries, J Stat Phys 65, (1991) 1269-1283.
[10] V. V. Anh, N. N. Leonenko, Spectral analysis of fractional kinetic equations with random data, J. Stat. Phys. 104, (2001) 1349-1387.
[11] A. Deppman, T. Frederico, E. Magias, D. P. Menezes, Fractal structure and non-extensive statistics, Entropy 20, (2018) 633.
[12] Y. Lu, O. Zhang, J. Zheng, C. Chang, H. Xie, Fractal model and lattice Boltzmann method for characterization of non-Darcy flow in rough fractures, Sci, Rep. 7, (2017) 41380.
[13] S. Lazzari, L. Nicoud, B. Jaquet, M. Lattuada, M. Morbidelli, Fractal-like structures in colloid science, Adv. Colloid Interface Sci. 235, (2016) 1-13.
[14] D. Chiappini, A. Donno, A comparison between different fractal grid generation methods coupled with lattice Boltzmann approach, AIP Conf. Proc. 1738 (2016) 270003.
[15] B. Yu, W. Liu, Fractal analysis of permeabilities for porous media, AIChE J. 50, (2004) 46-57.
[16] A. S. Balankin, O. Susarrey, C. A. Mora Santos, J. Patiño, A. Yoguez, E. I. García, Stress concentration and size effect in fracture of notched heterogeneous material, Phys. Rev. E83, (2001) 015101.

[17] A. S. Balankin, B. Espinoza, Map of fluid flow in fractal porous medium into fractal continuum flow, Phys. Rev. E85, (2002) 056314.
[18] K. R. Sreenivasan, Fractals in fluid mechanics, FRACTALS 2, (1994) 253-263.
[19] M. Ostoja-Starzewski, Extremum and variational principles for elastic and inelastic media with fractal geometries, Acta Mech. 205, (2009) 161-170.
[20] M. Zubair, M. J. Mughal, Q. A. Naqvi, The wave equation and general plane wave solutions in fractional space, Prog. Electromagnet. Res. Lett. 19, (2010) 137-146.
[21] A. S. Balankin, B. Mena, J. Patiño, D. Morales, Electromagnetic fields in fractal continua, Phys. Lett. A377, (2013) 783-788.
[22] R. A. El-Nabulsi, Path integral formulation of fractionally perturbed Lagrangian oscillators on fractal, J. Stat. Phys. 172, (2018) 1617-1640.
[23] R. A. El-Nabulsi, Emergence of quasiperiodic quantum wave functions in Hausdorff dimensional crystals and improved intrinsic Carrier concentrations, J. Phys. Chem. Sol. 127, (2019) 224-230.
[24] R. A. El-Nabulsi, On a new fractional uncertainty relation and its implications in quantum mechanics and molecular physics, Proc. Roy. Soc. A476, (2020) 20190729.
[25] R. A. El-Nabulsi, Inverse-power potentials with positive-bound energy spectrum from fractal, extended uncertainty principle and position-dependent mass arguments, Eur. Phys. J. P135, (2020) 683.
[26] R. A. El-Nabulsi, Dirac equation with position-dependent mass and Coulomb-like field in Hausdorff dimension, Few Body Syst. 61, (2020) 10.
[27] R. A. El-Nabulsi, Non-standard magnetohydrodynamics equations and their implications in sunspots, Proc. Royal Society A476, (2020) 20200190.
[28] A. G. Bershadskii, Large-scale fractal structure in laboratory turbulence, astrophysics, and the ocean, Soviet Physics Uspekhi. 33, (1990) 1073.
[29] R. A. El-Nabulsi, Fractional Navier-Stokes equation from fractional velocity arguments and its implications in fluid flows and microfilaments, Int. J. Nonlinear Sci. Numer. Simul. 20, (2019) 449-459.
[30] R. A. El-Nabulsi, Geostrophic flow and wind driven ocean currents based on dimensionality of the space medium, Pure Appl. Geophys. 176, (2019) 2739-2750.
[31] R. A. El-Nabulsi, Time-nonlocal kinetic equations, jerk and hyperjerks in plasmas and solar physics, Adv. Space Res. 61, (2018) 2914-2931.
[32] V. I. Abramenko, Multifractal analysis of solar magnetograms, Solar Phys. 228, (2005) 29.
[33] M. J. Aschwanden, P. D. Aschwanden, Solar flare geometries. I. The area fractal dimension, Astrophys. J. 674, (2008) 530-543.
[34] M. J. Aschwanden, P. D. Aschwanden, Solar flare geometries. II. The volume fractal dimension, Astrophys. J. 674, (2008) 544-553.
[35] A. A. Chernyshov, M. M. Mogilevsky, B. V. Kozelov, Use of fractal approach to investigate ionospheric conductivity in the auroral zone, J. Geophys. Res.: Space Phys. 118, (2013) 4108-4118.
[36] R. A. El-Nabulsi, Modifications at large distances from fractional and fractal arguments, FRACTALS 18, (2010) 185-190.
[37] A. S. Balankin, B. Mena, O. Susarrey, D. Samayoa, Steady laminar flow of fractal fluids, Phys. Lett. A381, (2017) 623-628.
[38] J. Cai, X. Hu, B. Xiao, Y. Zhou, W. Wei, Recent developments in fractal-based approach to nanofluids and nanoparticles aggregation, Int. J. Heat & Mass Transfer 105, (2017) 623-637.
[39] C. Q. Wu, H. J. Xu, C. Y. Zhao, A new fractal model on fluid flow/heat/mass transport in complex porous structures, Int. J. Heat & Mass Transfer 162, (2020) 120292.
[40] X. Shen, L. Li, W. Cui, Y. Feng, Improvement of fractal model for porosity and permeability in porous materials, Int. J. Heat & Mass Transfer 121, (2018) 1307-1315.
[41] X. Qin, J. Cai, P. Xu, S. Dai, Q. Gan, A fractal model of effective thermal conductivity for porous media with various liquid saturation, Int. J. Heat & Mass Transfer 128, (2019) 1149-1156.
[42] G. A. Losa, D. Merlini, T. F. Nonnenmacher, E. R. Weibel (Eds.), Fractals in Biology and Medicine, Mathematics and Biosciences in Interaction book series, Springer, 2005.
[43] N. C. Kendel, D. J. Walker, Fractals in the biological sciences, COENOSES 11, (1996) 77-100.
[44] B. J. West, A. L. Goldberger, Physiology in fractal dimensions, American Sci. 75, (1987) 354-365.
[45] G. Werner, Fractals in the nervous systems: conceptual implications for theoretical neurosciences, Front. Physiol. 1, (2015) 15.
[46] A. Di leva (Eds.), The Fractal Geometry of the Brain, Springer Series in Computational Neuroscience, Springer-Verlag, New York, 2016.
[47] H.-H. He, Fatalness of virus depends upon its cell fractal geometry, Chaos Solitons Fractals 38, (2008) 1390-1393.
[48] P. A. Naik, K. M. Owolabi, M. Yavuz, J. Zu, Chaotic dynamics of a fractional order HIV-1 model involving AIDS-related cancer cells, Chaos Solitons Fractals 140, (2020) 110272.
[49] J. W. Baish, R. K. Jain RK, Fractals and cancer, Cancer Res 60, (2000) 3683-3688.
[50] Q. Chen, N. Bao, Q. Yao, Z.-Y. Li, Fractal dimension: A complementary diagnostic indicator of osteoporosis to bone mineral density, Med. Hypoth. 116, (2018) 136-138.
[51] T. R. Nelson, Modeling of lung morphogenesis using fractal geometries. IEEE Trans. Med. Imag. 7, (1988) 321-327.
[52] W. Deering, B. J. West, Fractal physiology, IEEE Eng. Med. Bio. 11, (1992) 40-46.
[53] T. M. Griffith, Chaos and fractals in vascular biology, Vascular Med. Rev. 5, (1994) 161-182.
[54] M. Obert, P. Pfeifer, M. Sernetz, Microbial growth patterns described by fractal geometry, J. Bacteriology 172, (1990) 1180-1185.
[55] N. Dioguardi, F. Grizzi F, Fractal dimension exponent for quantitative evaluation of liver extracellular matrix in biopsy specimens. In: Losa GA, Merlini D, Nonnenmacher TF, Weibel ER (Eds.), Fractals in Biology and Medicine, Vol III, 113-120. Birkhäuser Press Basel, Switzerland, 2002.
[56] G. Landini, J. W. Rippin, Fractal dimensions of the epithelial-connective tissue interfaces in premalignant and malignant epithelial lesions of the floor of the mouth, Anal. Quant. Cytol. Histol 15, (1993) 144-149.
[57] A. J. Einstein, H. S. Wu, J. Gil, Fractal characterization of nuclear texture in breast cytology: frequency and spatial domain approaches. In: Losa GA, Merlini D, Nonnenmacher TF, Weibel ER (Eds.), Fractals in Biology and Medicine. Vol II, 190-.206. Basel, Switzerland, Birkhäuser Press, 1998.

[58] G. A. Losa, Fractals in Biology and Medicine. In: Meyers R (Ed.), Encyclopedia of Molecular Cell Biology and Molecular Medicine, Wiley-VCH Verlag, Berlin, 2012.
[59] G. Werner, Fractals in the nervous system: conceptual implications for theoretical neuroscience, Front Physiol. 1, (2010) 1-28.
[60] G. A. Losa, On the fractal design in human brain and nervous tissue, Appl. Math. 5, (2010) 1725-1732.
[61] F. Sepulcre J. Grau, M. Garcia-Bonafé, A. Moragas, Fractal approach to the study of chromatin texture. In: Losa GA, Merlini D, Nonnenmacher TF, Weibel ER (Eds.), Fractals in Biology and Medicine 4: 226-230. Birkhäuser Press. Basel, Switzerland, 2005.
[62] F. Marinelli, R. Santoro, N. M. Maraldi, Fractal analysis of heterochromatin nuclear domains in lymphocytes. In: Losa GA, Merlini D, Nonnenmacher TF, Weibel ER (Eds.), Fractals in Biology and Medicine 4: 220-225. Birkhäuser Press. Basel, Switzerland, 2005.
[63] S. S. Cross, A. J. G. McDonagh T. J. Stephenson, D. W. Cotton, J. C. Underwood, Fractal and integer-dimensional analysis of pigmented skin lesions, Am J Dermatol. 17, (1995) 374-378.
[64] Z. Liu, Z. Zhang, R. O. Ritchie, Structural orientation and anisotropy in biological materials: functional designs and mechanics, Adv. Func. Mater. 30, (2020) 1908121.
[65] G. Jacucci, O. D. Onelli, A. De Luca, J. Bertolotti, R. Sapienza, S. Vignolini, Coherent backscattering of light by an anisotropic biological network, Interface Focus 9, (2018) 20180050.
[66] Y.M. Efremov, N. Velay-Lizancos, C. J. Weaver, A. I. Athamneh, P. D. Zavattieri, D. M. Suter, A. Raman, Anisotropy vs isotropy in living cell indentation with AFM, Sci. Rep. 9, (2019) 5757.
[67] X. Chen, O. Korotkova, Optical beam propagation in soft anisotropic biological tissues, OSA Cont. 1, (2018) 1055-1067.
[68] C. Carrasco, A. Carreira, I. A. T. Schaap, P. A. Serena, J. Gómez-Herrero, M. G. Mateu, P. J. de Pablo, DNA-mediated anisotropic mechanical reinforcement of a virus, Proc. Nat. Acad. Sci. 103, (2006) 13706-13711.
[69] G. Lemineur, R. Harba, R. Jennane, A. Estrade, C. L. Benhamou, Fractal anisotropy measurement of bone texture radiographs, First International Symposium on Control, Communications and Signal Processing, 21-24 March 2004, Hammamet, Tunisia.
[70] C. Chappard, B. Brunet-Imbault, G. Lemineur, B. Giraudeau, A. Basillais, R. Harba, C. L. Benhamou, Anisotropy changes in post-menopausal osteoporosis: characterization by a new index applied to trabecular bone radiographic images, Osteoporos Int.16 (2005) 1193-1202.
[71] S. Dinicola, F. D'Anselmi, A. Pasqualato, S. Proietti, E. Lisi, A. Cucina, M. Bizzarri, A systems biology approach to cancer: fractals, attractors, and nonlinear dynamics, OMICS: A J. Integrative Biol. 15, (2011) 93-104.
[72] N. Bellomo, A. Bellouquid, M. Delitala, Methods and tools of mathematical kinetic theory towards modelling complex biological systems. In: C. Cercignani, E. Gabetta (Eds.) Transport Phenomena and Kinetic Theory. Modeling and Simulation in Science, Engineering and Technology, Birkhäuser Boston.
[73] L. M. Pereira, Fractal pharmacokinetics, Comp. Math. Meth. Medicine 11, (2010) 161-184.
[74] R.E. Marsh, T.A. Riauka, S.A. McQuarrie, Use of a simulated annealing algorithm to fit compartmental models with an application to fractal pharmacokinetics, J. Pharm. Pharmaceut. Sci. 10, (2007), 168-179.
[75] J. Li, M. Ostoja-Starzewski, Fractal solids, product measures and fractional wave equations, Proc. Roy. Soc. A465, (2009) 2521-2536.
[76] G. Jumarie, Table of some basic fractional calculus formulae derived from a modified Riemann-Liouville derivative for non-differentiable functions, Appl. Math. Lett. 22, (2008) 378-385.
[77] M. Ostoja-Starzewski, J. Li, P. N., Demmie, Continuum Homogenization of Fractal Media. In: G. Voyiadjis (eds) Handbook of Nonlocal Continuum Mechanics for Materials and Structures. Springer, Cham., 2019. https://doi.org/10.1007/978-3-319-58729-5_18.
[78] M. Ostoja-Starzewski, J. Li, H. Joumaa, P.N. Demmie, From fractal media to continuum mechanics, Z. Angew. Math. Mech. 94(5), (2014) 373-401.
[79] J. Li, M. Ostoja-Starzewski, Micropolar continuum mechanics of fractal media, Int. J. Eng. Sci. 49, (2011) 1302-1310.
[80] J. Li, M. Ostoja-Starzewski, Thermo-poromechanics of fractal media, Phil. Trans. Roy. Soc. A378, (2020) 20190288.
[81] M. Ostoja-Starzewski, Towards thermomechanics of fractal media, Z. Angew. Math. Mech. 58(6), (2007) 1085-1096.
[82] P. N. Demmie, M. Ostoja-Starzewski, Waves in fractal media, J. Elast. 104, (2011) 187-204.
[83] R. A. El-Nabulsi, Superconductivity and nucleation from fractal anisotropy and product-like fractal measure, Proc. Roy. Soc. A477, (2021) 20210065.
[84] R. A. El-Nabulsi, Thermal transport equations in porous media from product-like fractal measure, J. Therm. Stress. 44, (2021) 899-918.
[85] R. A. El-Nabulsi, On nonlocal fractal laminar steady and unsteady flows, Acta Mech. 232, (2021) 1413-1424.
[86] G. Jumarie, Table of some basic fractional calculus formulae derived from a modified Riemann-Liouville derivative for non-differentiable functions, Appl. Math. Lett. 22, (2008) 378-385.
[87] H. J. Morowitz, Energy Flow in Biology, New York, Academic Press, 1968.
[88] Y. Demirel, Thermodynamics and Biological Systems, in Nonequilibrium Thermodynamics 3rd Edition, Transport and Rate Processes in Physical, Chemical and Biological Systems, Chap. 11, (2014) 485-562.
[89] D. T. Haynie, Biological Thermodynamics, Cambridge University Press, Cambridge 2008.
[90] I, Lamprecht, A. I. Zotin (Eds.), Thermodynamics and Kinetic of Biological Processes, De Gruyter, 1982. https://doi.org/10.1515/9783110845914.
[91] U. Lucia, Bioengineering thermodynamics of biological cells, Theor. Biol. Med. Mod. 12, (2015) 29.
[92] R. Davireddy, Thermodynamics analysis of biological systems, J. Thermodyn. Catalys. 3, (2012) 2.
[93] H.-W. Huang, T.-L. Horng, Bioheat Transfer and Thermal Heating for Tumor Treatment; Chap. 1 in Heat Transfer and Fluid Flow in Biological Processes, 2015, 1-42, Academic Press, ScienceDirect, Elsevier.
[94] M. Paruch, Mathematical modeling of breast tumor destruction using fast heating during radiofrequency ablation, Materials 13. (2020) 136.
[95] Y. Xu, S. Long, Y. Yang, F. Zhou, N. Dong, K. Yan, B. Wang, Y. Zeng, N. Du, X. Li, W. R. Chen, Mathematical simulation of temperature distribution in tumor tissue and surrounding healthy tissue treated by laser combined with indocyanine green, Theor. Biol. Med. Mod. 16, (2012) 12.

[96] S. Liu, A. Doughty, C. West, Z. Tang, F. Zhou, W. R. Chen, Determination of temperature distribution in tissue for interstitial cancer photothermal therapy, Int. J. Hyperthermia 34, (2018) 756-763.
[97] J. W. Baish, R. K. Jain, Fractals and Cancer, Cancer Res. 60, (2000) 3683-2688.
[98] M. Bizzarri, A. Giuliani, A. Cucina, F. D'Anselmi, A. M. Soto, C. Sonnenschein, Fractal analysis in a systems biology approach to cancer, Sem. Cancer Biol. 21, (2011) 175-182.
[99] P. Hamill, A student's guide to Lagrangians and Hamiltonians, Cambridge University Press, Cambridge, 2014.
[100] J. D. Anderson, Jr. Fundamentals of Aerodynamics, 2nd Edition McGraw-Hill, New York, 1991.
[101] J. D. Anderson, Jr., Modern Compressible Flow: With Historical Perspective, 2nd Edition McGraw-Hill, New York, 1990.
[102] H. H. Pennes, Analysis of tissue and arterial blood temperatures in the resting human forearm, J. Appl. Physiol. 1, (1948) 93-122.
[103] L. Zhu, T. Schappeler, C. Cordero-Tumangday, A. J. Rosengart, Thermal interactions between blood and tissue: development of a theoretical approach in predicting body temperature during blood cooling/rewarming, Adv. Numer. Heat Transf. 3, (2009) 197-219.
[104] M. Kutz, Biomedical Engineering and Design Handbook, Volume 1, McGraw Hill, New York, US, 2009.
[105] E. A. Repaksy, S. S. Evans, M. W. Dewhirst, Temperature matters! And why it should mater to tumor immunologists, Cancer Immunol. Res. 1, (2013) 210-216.
[106] M. Paruch, Mathematical modeling of breast tumor destruction using fast heating during radiofrequency ablation, Materials 13, (2020) 136.
[107] Y. Qin, K. Wu, Numerical solution of fractional bioheat equation by quadratic spline collocation method, J. Nonlinear Sci. Appl. 9, (2016) 5061-5072.
[108] J. Singh, P. K. Gupta, K. N. Rai, Solution of fractional bioheat equations by finite difference method and HPM, Math. Comput. Model. 54, (2011) 2316-2325.
[109] J. Okajima, S. Maruyama, H. Takeda, A. Komiya, Dimensionless solutions and general characteristics of bioheat transfer during thermal therapy, J. Therm. Biol. 34, (2009) 377-384.
[110] H. W. Huang, C. L. Chan, R. B. Roemer, Analytical solutions of Pennes bio-heat transfer equation with a blood vessel, Trans. ASME116, (1994) 208-212.
[111] M. A. Giordano, G. Gutierrez, C. Rinaldi, Fundamental solutions to the bioheat equation and their application to magnetic fluid hyperthermia, Int. J. Hyperthermia 26, (2010) 475-485.
[112] A. Andreozzi, L. Brunese, M. Iasiello, C. Tucci, F. P. Vanoli, Bioheat transfer in a spherical biological tissue: a comparison among various models, J. Phys.: Conf. Ser. 1224, (2019) 012001.
[113] T.-C. Shih, H.-S. Kou, C.-T. Liauh, W.-L. Lin, Thermal models of bioheat transfer equations in living tissue and thermal dose equivalence due to hyperthermia, Biomed. Eng. Appl. Basis Comm. 14, (2002) 86-96.
[114] A. Lozano III, J. C. Hayes, L. M. Compton, J. Azarnoosh, F. Hassanipour, Determining the thermal characteristics of breast cancer based on high-resolution infrared imaging, 3D breast scans, and magnetic resonance imaging, Sci. Rep. 10, (2020) 10105.
[115] J. H. Lienhard IV, J. H. Lienhard V, A Heat Transfer Textbook, 5th Edition, MIT Press, Massachusetts, Boston, US, 2019.
[116] S. Hossain, F. Mohammadi, One-dimensional steady-state analysis of bioheat transfer equation: tumour parameters assessment for medical diagnosis application, In: Proceedings 6th international multi-conference on engineering and technological innovation (IMETI 2013), pp 26-30.
[117] L. K. Foong, M. Zarringhalam, D. Toghraie, N. Izadpanahi, S.-R. Yan, S. Rostami, Numerical study for blood rheology inside an artery: the effects of stenosis and radius in the flow behavior, Comp. Meth. Program. Biomed. 193, (2020) 105457.
[118] D. Ambrosi, M. Ben Amar, C. J. Cryon, A. DeSimone, A. Goriely, J. D. Humphrey, E. Kuhl, Growth and remodeling of living tissues: perspectives, challenges and opportunities, J. Roy. Soc. Interface 16, (2021) 20190233.
[119] A. Lakhssassi, E. Kengne, H. Semmaoui, Modified Pennes' equation modelling bio-heat transfer in living tissues: analytical and numerical analysis, Nat. Sci. 2, (2010) 1375-1385.
[120] S. Ozen, S. Helhei, S. Bilgin, Temperature and burn injury prediction of human skin exposed to microwaves: a model analysis, Radiat. Environ. Biophys. 50, (2011) 483-489.
[121] Z. Vujaskovic, J. M. Poulson, A. A. Gaskin, D. E. Thrall, R. L Page, H. C. Charles, J. R. MacFall, D. M. Brizel, R. E. Meyer, D. M. Prescott, T. V. Samulski, M. W. Dewhirst, Temperature-dependent changes in physiologic parameters of spontaneous canine soft tissue sarcomas after combined radiotherapy and hyperthermia treatment, Int. J. Radiat. Oncol. Biol. Phys. 46, (2000) 179-185.
[122] E. L. Jones L. R. Prosnitz, M. W. Dewhirst, P. K. Marcom, P. H. Hardenbergh, L. B. Marks, D. M. Brizel, Z. Vujaskovic, Thermochemoradiotherapy improves oxygenation in locally advanced breast cancer, Clin. Cancer Res. 10, (2004) 4287-4293.
[123] P. J. Brown, R. A. Dove, C. S. Tuffnell, R. P. Ford, Oscillations of body temperature at night, Arch. Dis. Child 67, (1992) 1255-1258.
[124] J. Rodenfels, K. M. Neugebauer, J. Howard, Heat oscillations driven by the embryonic cell cycle reveal the energetic costs of signaling, Develop. Cell 48, (2019) 646-658.e6.
[125] F. Xu, S. Moon, Z. Zhang, L. Shao, Y. S. Song, U. Demicri, Multi-scale heat and mass transfer modelling of cell and tissue cryopreservation, Philos. Trans. A. Math. Phys. Eng. Sci. 13, (2010) 561-583.
[126] C. Cattaneo, A form of heat-conduction equations which eliminates the paradox of instantaneous propagation, Compt. Rendus. 247 (1958) 431.
[127] P. Vernotte, Les paradoxes de la théorie continue de l'équation de la chaleur, Compt. Rendu. 246 (1958) 3154–3155.
[128] W. Kaminsk, Hyperbolic heat conduction equation for materials with a nonhomogeneous inner structure, J. Heat Transf. 112, (1990) 555-560.
[129] K. K. Tamma, X. Zhou, Macroscale and microscale thermal transport and thermo-mechanical interactions: some noteworthy perspectives, J. Therm. Stress. 21, (1998) 405-449.
[130] D. Maillet, A review of the models using the Cattaneo and Vernotte hyperbolic heat equation and their experimental validation, Int. J. Therm. Sci. 139, (2019) 424-432.
[131] J.-L. Auriault, Cattaneo–Vernotte equation versus Fourier thermoelastic hyperbolic heat equation, Int. J. Eng. Sci. 101, (2016) 45-49.
[132] T.-C. Shih, P. Yuan, W.-L. Lin, H.-S. Kou, Analytical solutions of the Pennes bioheat transfer equation with sinusoidal heat flux condition on skin surface, J. Med. Eng. Phys. 29, (2007) 946-953.

[133] A. A. Sagaidachnyi, D. A. Usanov, A. V. Skripal, A. V. Fomin, Correlation of skin temperature and blood flow oscillations, Proceedings Vol. 8337, Saratov Fall Meeting 2011: Optical Technologies in Biophysics and Medicine XIII; 83370A, 2012; http://doi.org/10.1117/12.955156.
[134] J. Li, M. Ostoja-Starzewski, Thermo-poromechanics of fractal media, Phil. Trans. R. Soc. A 378, (2020) 20190288.
[135] G. C. Shit, A. Bera, Temperature response in a living tissue with different heating source at the skin surface under relaxation time, Int. J. Appl. Comput. Math. 3, (2017) 381-394.
[136] T. F. Kamalov, Instability criterion and uncertainty relation, J. Phys. Conf. Ser. 1557(1), (2020) 012003.
[137] X. Li, Y. Li, P. Luo, X. Tian, Relationship between the nonlocal effect and lagging behavior in bioheat transfer, J. Heat Transf. 143, (2021) 051201.
[138] J. A. K. Suykens, J. P. L. Vandewalle (Eds.), Nonlinear Modeling: Advanced Black-Box Techniques, Springer, 1998.
[139] J. A. K. Suykens, Extending Newton's law from nonlocal-in-time kinetic energy, Phys. Lett. A373, (2009) 1201-1211.
[140] J. Zhang, S. Chauhan, Real-time computation of bio-heat transfer in the fast explicit dynamics finite element algorithm (FED-FEM) framework, Numer. Heat Transf. B: Fund. 75, (2009) 217-238.